

Fractal analysis of canard cycles and slow-fast Hopf points in piecewise smooth Liénard equations

Renato Huzak¹, Ansfried Janssens*², Otavio Henrique Perez³, and
Goran Radunović⁴

^{1,2,3}Hasselt University, Campus Diepenbeek, Agoralaan Gebouw D,
3590 Diepenbeek, Belgium

³Universidade de São Paulo (USP), Instituto de Ciências
Matemáticas e de Computação (ICMC). Avenida Trabalhador São
Carlense, 400, CEP 13566-590, São Carlos, São Paulo, Brazil.

⁴University of Zagreb, Faculty of Science, Horvatovac 102a, 10000
Zagreb, Croatia

¹renato.huzak@uhasselt.be

²ansfried.janssens@uhasselt.be

³otavio.perez@icmc.usp.br

⁴goran.radunovic@math.hr

Abstract

The main goal of this paper is to give a complete fractal analysis of piecewise smooth (PWS) slow-fast Liénard equations. For the analysis, we use the notion of Minkowski dimension of one-dimensional orbits generated by slow relation functions. More precisely, we find all possible values for the Minkowski dimension near PWS slow-fast Hopf points and near bounded balanced crossing canard cycles. We study fractal properties of the unbounded canard cycles using PWS classical Liénard equations. We also show how the trivial Minkowski dimension implies the non-existence of limit cycles of crossing type close to Hopf points. This is not true for crossing limit cycles produced by bounded balanced canard cycles, i.e. we find a system undergoing a saddle-node bifurcation of crossing limit cycles and a system without limit cycles (in both cases, the Minkowski dimension is trivial). We also connect the Minkowski dimension with upper bounds for the number of limit cycles produced by bounded canard cycles.

Keywords: canard cycles; Minkowski dimension; piecewise smooth slow-fast Hopf point; piecewise smooth slow-fast Liénard equations; slow relation function
2020 Mathematics Subject Classification: 34E15, 34E17, 34C40, 28A80, 28A75

*Corresponding author, ansfried.janssens@uhasselt.be

Contents

1	Introduction	2
2	Minkowski dimension	5
3	PWS slow-fast Liénard systems and statement of results	6
3.1	Fractal analysis of the PWS slow-fast Hopf point	8
3.2	Fractal analysis of bounded balanced canard cycles	10
3.3	Fractal analysis of PWS classical Liénard equations near infinity	11
4	Proof of Theorems 3.1–3.4	13
4.1	Proof of Theorems 3.1 and 3.2	13
4.2	Proof of Theorem 3.3	16
4.3	Proof of Theorem 3.4	17
4.3.1	Poincaré–Lyapunov compactification	17
4.3.2	Fractal Analysis Near Infinity	18
4.3.3	Completing the proof of Theorem 3.4	22
5	Crossing limit cycles and Minkowski dimension	23
5.1	Limit cycles near the PWS Hopf point	23
5.1.1	Dynamics in the chart $\bar{y} = 1$	24
5.1.2	Dynamics in the chart $\bar{\epsilon} = 1$	24
5.2	Limit cycles near bounded canard cycles	26
5.3	Limit cycles near the unbounded canard cycle	27

1 Introduction

The main purpose of this paper is to give a fractal classification of piecewise smooth (PWS) continuous slow-fast Liénard equations

$$\begin{cases} \dot{x} = y - F(x), \\ \dot{y} = \epsilon G(x), \end{cases} \quad (1)$$

with

$$F(x) = \begin{cases} F_-(x), & x \leq 0, \\ F_+(x), & x \geq 0, \end{cases} \quad G(x) = \begin{cases} G_-(x), & x \leq 0, \\ G_+(x), & x \geq 0, \end{cases} \quad (2)$$

where $\epsilon \geq 0$ is a singular perturbation parameter kept small, F_{\pm} and G_{\pm} are C^{∞} -smooth functions, $F_{\pm}(0) = F'_{\pm}(0) = 0$ and $G_{\pm}(0) = 0$. The set $\Sigma = \{x = 0\}$ is called the switching line or switching manifold. For the classification, we will use the notion of Minkowski dimension (always equal to the box dimension [13, 40]) of one-dimensional monotone orbits generated by so-called slow relation (or entry-exit) function (see Section 3). We refer to [1, 7, 10] and references therein for the definition of the notion of slow relation function in smooth planar slow-fast systems.

One of the important properties of such one-dimensional monotone orbits is their density. The density is usually measured by calculating the length of δ -neighborhood of orbits as $\delta \rightarrow 0$ and comparing the length with δ^{1-s} , $0 \leq$

$s \leq 1$. In this way we obtain the Minkowski dimension of orbits, taking values between 0 and 1 (for more details, see Section 2). The bigger the Minkowski dimension of the orbits, the higher the density of orbits. Following [12, 32, 44], the Minkowski dimension of orbits generated by the Poincaré map near foci, limit cycles, homoclinic loops, etc., is closely related to the number of limit cycles produced in bifurcations (roughly speaking, the bigger the Minkowski dimension, the more limit cycles can be born).

Similarly, in smooth planar slow-fast systems, the Minkowski dimension of orbits generated by a slow relation function plays an important role in detecting the codimension of singular Hopf bifurcations in a coordinate-free way [7], finding the maximum number of limit cycles produced by canard cycles [20, 21, 24], etc. For a more detailed motivation we refer the interested reader to [7, Section 1] and [8, Section 1]. Since these papers deal only with smooth slow-fast systems, it is natural to ask whether we can use similar methods to study fractal properties of *PWS slow-fast systems*.

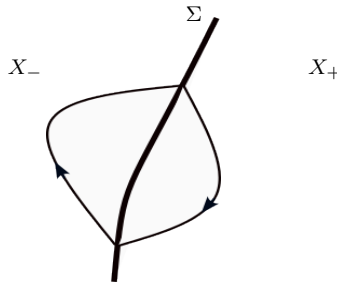


Figure 1: A crossing periodic orbit where Σ is the switching manifold.

Piecewise smooth systems [15] are an active field of recent research. The determination of crossing limit cycles, for example, is an important problem in PWS theory in the plane (see [3, 17, 19, 28, 29] and references therein). Such cycles intersect the switching manifold Σ at points where the vector fields X_- and X_+ point in the same direction relative to Σ (see Figure 1).

In this paper we are interested in the following limit periodic sets of the PWS slow-fast system (1) (we also refer to Figure 2 in Section 3). Assume that the curve of singularities of (1) contains a normally attracting branch $\{y = F_+(x), x > 0\}$ and a normally repelling branch $\{y = F_-(x), x < 0\}$. Then the balanced canard cycle $\Gamma_{\hat{y}}$, with $\hat{y} > 0$ when $\epsilon = 0$, consists of a portion of the normally attracting branch, a portion of the normally repelling branch and a horizontal fast orbit at level $y = \hat{y}$. These canard cycles may produce crossing limit cycles after a perturbation of (1) if the slow dynamics of (1) defined along the curve of singularities points from the attracting branch to the repelling branch and it has a regular extension through the origin $(x, y) = (0, 0)$ (see Section 5). This can be done by merging two smooth slow-fast Hopf points [11] into a so-called PWS slow-fast Hopf point located at the origin $(x, y) = (0, 0)$ (see assumption (4) in Section 3). The PWS slow-fast Hopf point is the limit of $\Gamma_{\hat{y}}$ when $\hat{y} \rightarrow 0$. If $\hat{y} \rightarrow \infty$, we can have an unbounded canard cycle, which will be denoted by Γ_∞ , consisting of the curve of singularities and a part at infinity (see Section 3.3).

The main goal is to give a *complete* fractal classification (i.e., we find all possible Minkowski dimensions) of the PWS slow-fast Hopf point and $\Gamma_{\hat{y}}$ described in the previous paragraph, related to the PWS continuous Liénard family (1). The fractal classification of the PWS slow-fast Hopf point is given in Theorems 3.1 and 3.2 in Section 3.1, whereas the possible Minkowski dimensions of $\Gamma_{\hat{y}}$ are given in Theorem 3.3 in Section 3.2. We assume that $\Gamma_{\hat{y}}$ is balanced, that is, the slow divergence integral computed along the portion of the curve of singularities contained in $\Gamma_{\hat{y}}$ is zero (see Section 3.2 and [10]). In Theorem 3.4 in Section 3.3 we compute Minkowski dimensions near Γ_{∞} when (1) is a PWS classical Liénard system (that is, F_{\pm} are polynomials of degree $n+1$, $n \geq 1$, and G_{\pm} are linear). Theorems 3.1 to 3.4 are proven in Section 4.

In Section 5, the link between the Minkowski dimensions computed in Section 4 and the number of crossing limit cycles of a perturbation of (1) near $\Gamma_0 = \{(0,0)\}$, $\Gamma_{\hat{y}}$ and Γ_{∞} is addressed (see system (49) in Section 5). We focus our study to the case in which the Minkowski dimensions are trivial (that is, equal zero). Geometrically speaking, close to a PWS Hopf point, trivial Minkowski dimension of orbits tending to Γ_0 means that the connection between center manifolds are broken in the blow-up locus, so we cannot expect crossing limit cycles (see Section 5.1 and Figure 4). However, trivial Minkowski dimension of orbits tending to $\Gamma_{\hat{y}}$ does not imply the absence of limit cycles. Indeed, we present an example in which the system undergoes a saddle-node bifurcation of limit cycles (see Section 5.2). Finally, in Section 5.3 we give examples in which the Minkowski dimension of orbits tending to Γ_{∞} is trivial, but, nevertheless, one can expect crossing limit cycles. The number of limit cycles related to higher Minkowski dimensions is a topic for future study (see Remark 6 in Section 5 for some results in that direction).

In the smooth setting, that is, when the functions F and G in (2) are C^{∞} -smooth, we deal with a smooth slow-fast Hopf point at the origin $(x, y) = (0, 0)$ and the following discrete set of values of the Minkowski dimension can be produced (see [7]): $\frac{1}{3}, \frac{3}{5}, \frac{5}{7}, \dots, 1$. From these values, which can be computed numerically [7], we can read upper bounds for the number of limit cycles produced by the smooth slow-fast Hopf point (for more details see [7, Theorem 3.4]). Theorems 3.1 and 3.2 imply that the PWS slow-fast Hopf point produces infinitely many new values: $0, \frac{1}{2}, \frac{2}{3}, \frac{3}{4}, \dots$. We strongly believe that they give information about the number of limit cycles produced by the PWS slow-fast Hopf point. This is a topic of further study.

Similarly, besides old values of the Minkowski dimension when F is a polynomial of even degree $n+1$ and G is linear ($\frac{1}{2}, \frac{3}{4}, \dots, \frac{n-2}{n-1}$, see [8, Remark 1]), in the piecewise smooth setting, Γ_{∞} produces the following new values: $0, \frac{4}{5}, \frac{6}{7}, \dots, \frac{n-1}{n}$. We refer to Theorem 3.4 for more details.

The main reason why we assume that F_{\pm} and G_{\pm} are C^{∞} -smooth is because we want to detect all possible Minkowski dimensions of orbits. We need higher-order Taylor expansions (i.e., higher degrees of smoothness of F_{\pm} and G_{\pm}) in order to find larger Minkowski dimensions of orbits (see Sections 4.1 and 4.2).

Let us highlight the differences between our approach and those already presented in the literature concerning PWS slow-fast systems. In [4, 38] the authors studied the existence of crossing canard limit cycles in piecewise smooth Liénard equations, in such a way that the origin is a corner point of the critical manifold (or curve of singularities) positioned in Σ , in the sense that $F'(0)$ in (1) is not well defined. Moreover, the critical manifold of the models studied in

such references presents a “van der Pol - like” shape. On the other hand, in [9] the authors also address the existence of canard limit cycles, but considering a three-zoned piecewise smooth Liénard equation instead. In [2, 14] the authors studied the existence of canard cycles in four-zoned and three-zoned piecewise linear (PWL) systems, respectively.

In all those references, [2, 4, 9, 14, 38], the authors fixed a linear function G in (1) (that is, $G_- = G_+$) and defined F in a piecewise smooth way. Moreover, in their models, the critical manifold loses smoothness in the intersection with the switching manifold. On the other hand, in this paper, we allow both F and G to be defined in a piecewise smooth way. Moreover, in the study of the Hopf point and the bounded canard cycle, we do not require G to be linear. In addition, the intersection between the critical manifold and Σ is not a corner point. Finally, our main tools are Fractal Geometry, Slow Divergence Integrals and Slow-Relation Functions, which were not used in those previous references.

A connection between sliding canard cycles in regularized PWS systems and the slow divergence integral can be found in [23].

2 Minkowski dimension

Let $U \subset \mathbb{R}^N$ be a bounded set. One defines its δ -neighborhood (or δ -parallel body) as $U_\delta := \{x \in \mathbb{R}^N \mid \text{dist}(x, U) \leq \delta\}$, where $\text{dist}(x, U)$ denotes the euclidean distance from x to the set U . Denote the Lebesgue measure of U_δ by $|U_\delta|$. For $s \geq 0$, we introduce the lower s -dimensional Minkowski content of U

$$\mathcal{M}_*^s(U) = \liminf_{\delta \rightarrow 0} \frac{|U_\delta|}{\delta^{N-s}},$$

and similarly, the upper s -dimensional Minkowski content $\mathcal{M}^{*s}(U)$ (replacing $\liminf_{\delta \rightarrow 0}$ with $\limsup_{\delta \rightarrow 0}$ above). We then define the lower and upper Minkowski (or box-counting, since they always coincide) dimensions of U as:

$$\underline{\dim}_B U = \inf\{s \geq 0 \mid \mathcal{M}_*^s(U) = 0\}, \quad \overline{\dim}_B U = \inf\{s \geq 0 \mid \mathcal{M}^{*s}(U) = 0\}.$$

When the upper and lower dimensions coincide, we refer to their common value as the Minkowski dimension of U , denoted by $\dim_B U$. For a comprehensive treatment of Minkowski dimension, we direct the reader to [13, 40] and the references therein. Furthermore, if there exists a d such that $0 < \mathcal{M}_*^d(U) \leq \mathcal{M}^{*d}(U) < \infty$, we say that U is Minkowski nondegenerate in which case, $d = \dim_B U$ necessarily.

Consider a bi-Lipschitz mapping $\Phi : U \subset \mathbb{R}^N \rightarrow \mathbb{R}^{N_1}$, i.e., there exists a constant $\rho > 0$ such that

$$\rho \|x - y\| \leq \|\Phi(x) - \Phi(y)\| \leq \frac{1}{\rho} \|x - y\|$$

for all $x, y \in U$. Then it is well-known that

$$\underline{\dim}_B U = \underline{\dim}_B \Phi(U), \quad \overline{\dim}_B U = \overline{\dim}_B \Phi(U).$$

Moreover, if U is Minkowski nondegenerate, then $\Phi(U)$ is also Minkowski nondegenerate (refer to [42, Theorem 4.1]).

We also introduce here some notation used throughout this paper. For two sequences of positive real numbers $(a_l)_{l \in \mathbb{N}}$ and $(b_l)_{l \in \mathbb{N}}$ converging to zero, we write $a_l \simeq b_l$ as $l \rightarrow \infty$ if there exists a small positive constant ρ such that $\frac{a_l}{b_l} \in [\rho, \frac{1}{\rho}]$ for all $l \in \mathbb{N}$.

Note that the Minkowski dimension has proven to be a useful tool in fractal analysis of various dynamical systems which enables one to extract information about the cyclicity of the system directly from analyzing the Minkowski dimension of one of its orbits [36, 43] or even by looking just at the Minkowski dimension of a discrete orbit generated by the suitable Poincaré map [12, 44] or even Dulac map [31]. Furthermore, since the Minkowski dimension is always equal to the box dimension [13] which can be effectively computed numerically [5, 7, 16, 33–35, 39, 41], it is natural to expect that numerical methods for determining cyclicity via the Minkowski dimension can be developed which puts further value to the results in our paper.

It was also shown that the Minkowski dimension is useful in providing a novel tool for formal and analytic classification of parabolic diffeomorphism in the complex plane. Even for the formal classification of parabolic germs one first needs to extend the definition of the Minkowski dimension either as in [37] or alternatively also look at higher order terms in the asymptotic series of the δ -neighborhood of the orbit as δ tends to zero [30]. The latter approach is closely connected to the theory of complex (fractal dimensions) and associated fractal zeta functions introduced by Lapidus and van Frankenhuijsen [27] for subsets of \mathbb{R} and then extended to the general case of subsets of \mathbb{R}^N in [26]. Furthermore, in order to tackle the analytic classifications of parabolic germs one needs to further extend and adapt the theory of complex dimensions as in [25].

Finally, note that, in contrast to the Minkowski dimension, the Hausdorff dimension would not extract us any relevant information from orbits of dynamical systems. The reason for this stems from the countable stability of the Hausdorff dimension which renders all of the orbits of the dynamical systems to have either dimension 1 in the continuous case, or 0 in the discrete case. On the other hand, the lack of the countable stability of the Minkowski dimension is exactly the reason which makes it interesting and useful for the fractal analysis of orbits of dynamical systems. Of course, as it is well known, an attractor of a dynamical system can have nontrivial Hausdorff dimension (strange attractors such as Lorenz or Hénon, etc). However, in all cases mentioned above, as well as in this paper the attractor is either a point (possibly at infinity) or a piecewise smooth curve, hence of trivial Hausdorff dimension.

3 PWS slow-fast Liénard systems and statement of results

We consider a PWS slow-fast Liénard equation

$$X_- : \begin{cases} \dot{x} = y - F_-(x), \\ \dot{y} = \epsilon G_-(x), \end{cases} \quad \text{for } x \leq 0, \quad X_+ : \begin{cases} \dot{x} = y - F_+(x), \\ \dot{y} = \epsilon G_+(x), \end{cases} \quad \text{for } x \geq 0, \quad (3)$$

where $0 < \epsilon \ll 1$ is a singular perturbation parameter and F_\pm and G_\pm are C^∞ -smooth functions. We assume that X_- and X_+ have a slow-fast Hopf point at

the origin $(x, y) = (0, 0)$, that is, they satisfy (see also [11, Definition 1.1])

$$F_{\pm}(0) = F'_{\pm}(0) = G_{\pm}(0) = 0, \quad F''_{\pm}(0) > 0 \text{ and } G'_{\pm}(0) < 0. \quad (4)$$

We say that system (3) satisfying (4) has a PWS slow-fast Hopf point at $(x, y) = (0, 0)$. For $\epsilon = 0$, system (3) has the curve of singularities

$$S = \{(x, F_-(x)) \mid x < 0\} \cup \{(0, 0)\} \cup \{(x, F_+(x)) \mid x > 0\}.$$

We denote by S_- (resp. S_+) the branch of S contained in $x < 0$ (resp. $x > 0$). We refer to Figure 2. From (4), it follows that (near the PWS slow-fast Hopf point) S_- (resp. S_+) consists of normally repelling (resp. attracting) singularities. Then we can define the slow vector field of (3) along S , near $(x, y) = (0, 0)$, as the following PWS vector field

$$X_-^s : \frac{dx}{d\tau} = \frac{G_-(x)}{F'_-(x)}, \quad x \leq 0, \quad X_+^s : \frac{dx}{d\tau} = \frac{G_+(x)}{F'_+(x)}, \quad x \geq 0, \quad (5)$$

where $\tau = \epsilon t$ is the slow time (t denotes the fast time in (3)). Its flow is called the slow dynamics. Using (4), it is clear that (5) has a removable singularity in $x = 0$ and the slow dynamics is regular and it points from the attracting branch S_+ to the repelling branch S_- . Notice that the slow vector field [6, Chapter 3] of the smooth slow-fast system X_- (resp. X_+) along S_- (resp. S_+) is given by X_-^s (resp. X_+^s) defined in (5). See also [22].

In this paper we focus on fractal analysis of 3 different types of limit periodic sets of (3), for $\epsilon = 0$ (see Figure 2): (a) the PWS slow-fast Hopf point at $(x, y) = (0, 0)$ (Section 3.1), (b) bounded canard cycles $\Gamma_{\hat{y}}$, $\hat{y} > 0$, consisting of the fast horizontal orbit of (3) passing through the point $(0, \hat{y})$ and the portion of S between the ω -limit point $(\omega(\hat{y}), \hat{y}) \in S_+$ and the α -limit point $(\alpha(\hat{y}), \hat{y}) \in S_-$ of that orbit (Section 3.2), and (c) an unbounded canard cycle consisting of S and a part at infinity (Section 3.3). When we deal with the canard cycles in (b) and (c), we need some additional assumptions on the functions F_{\pm} and G_{\pm} :

$$F'_-(x) < 0, \quad G_-(x) > 0, \quad \forall x \in L_-, \quad F'_+(x) > 0, \quad G_+(x) < 0, \quad \forall x \in L_+, \quad (6)$$

where $L_- = [\alpha(\hat{y}), 0[$ and $L_+ =]0, \omega(\hat{y})]$ in case (b) and $L_- =]-\infty, 0[$ and $L_+ =]0, \infty[$ in case (c). The assumptions in (6) imply that the slow vector field (5) is well-defined on the closure $\overline{L_- \cup L_+}$ and it has no singularities.

The canard cycles considered throughout this paper are, in fact, crossing canard cycles according to Filippov's convention [15]. More precisely, when one deals with piecewise smooth vector fields, one can define sewing and sliding regions in the switching locus $\Sigma = \{x = 0\}$, which are given by

$$\begin{aligned} \Sigma^w &= \{(x, y) \in \Sigma ; (y - F_-(x))(y - F_+(x)) > 0\}, \\ \Sigma^s &= \{(x, y) \in \Sigma ; (y - F_-(x))(y - F_+(x)) < 0\}, \end{aligned}$$

respectively. It follows directly from assumptions in (4) that $\Sigma^s = \emptyset$ and $\Sigma^w = \Sigma \setminus \{0\}$.

Slow divergence integrals (see [6, Chapter 5] and [22]) play an important role in fractal analysis of the limit periodic sets defined above. The slow divergence

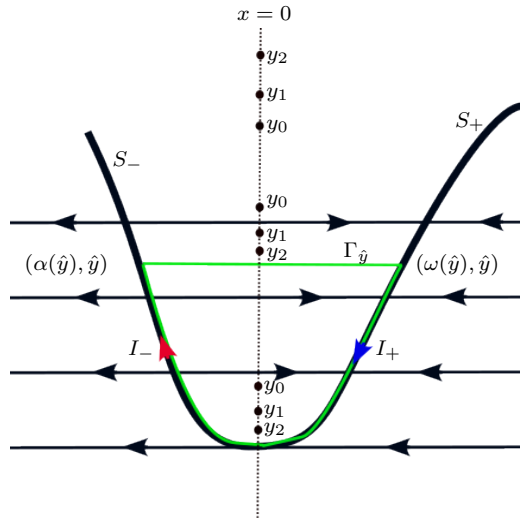


Figure 2: The phase portrait of (3) for $\epsilon = 0$, with indication of the slow dynamics along the curve of singularities S . Orbits $U = \{y_0, y_1, \dots\}$ generated by the slow relation function H can converge to the PWS slow-fast Hopf point $(x, y) = (0, 0)$, a canard cycle $\Gamma_{\hat{y}}$ (green) or the unbounded canard cycle.

integral of X_- (resp. X_+) associated with the segment $[\alpha(y), 0]$ (resp. $[0, \omega(y)]$) are given by

$$I_-(y) := - \int_{\alpha(y)}^0 \frac{F'_-(x)^2}{G_-(x)} dx < 0, \quad I_+(y) := - \int_{\omega(y)}^0 \frac{F'_+(x)^2}{G_+(x)} dx < 0, \quad (7)$$

respectively, where $\alpha(y) < 0$, $F_-(\alpha(y)) = y$, $\omega(y) > 0$ and $F_+(\omega(y)) = y$. The argument $y > 0$ of I_{\pm} is close to $y = 0$ (case (a)), $y = \hat{y}$ (case (b)) or large enough (case (c)). It is not difficult to see that $I'_{\pm}(y) < 0$ and $I_{\pm}(y) \rightarrow 0$ as y tends to 0. We also define

$$I(y) := I_+(y) - I_-(y). \quad (8)$$

Our goal is to compute the Minkowski dimension of orbits generated by so-called slow relation function H (or its inverse) defined by

$$I_-(H(y)) = I_+(y). \quad (9)$$

See [10, Section 4] for more details concerning the slow relation function in the framework of smooth slow-fast systems. We denote by U the orbit of $y_0 > 0$ by H , that is, $U = \{y_l = H^l(y_0) \mid l \in \mathbb{N}\}$, in which H^l is the l -fold composition of H . In Section 3.1 (resp. Sections 3.2 and 3.3) we consider orbits U that tend to 0 (resp. \hat{y} and ∞).

3.1 Fractal analysis of the PWS slow-fast Hopf point

In this section we consider (3) in a small neighborhood of the PWS slow-fast Hopf point $(x, y) = (0, 0)$. Since the integrals I_- and I_+ are (continuous)

decreasing functions and tend to zero as $y \rightarrow 0$, it is clear that, for each $y > 0$ small enough, there is a unique $H(y) > 0$ such that (9) holds. Analogously, for each $y > 0$ small enough, there is a unique $H^{-1}(y) > 0$ such that $I_-(y) = I_+(H^{-1}(y))$. Furthermore, we also assume that there is a small $y^* > 0$ such that I defined in (8) is nonzero in the open interval $]0, y^*[$.

Now, given $y_0 \in]0, y^*[$, if $I > 0$ (resp. $I < 0$) on $]0, y^*[$ then we denote by U the orbit $\{y_0, y_1, y_2, \dots\}$ defined by

$$I_-(y_{l+1}) = I_+(y_l) \quad (\text{resp. } I_-(y_l) = I_+(y_{l+1})), \quad \text{with } l \geq 0.$$

Observe that U is the orbit of y_0 by H (resp. H^{-1}) and it tends monotonically to 0 as $l \rightarrow \infty$. Conversely, if $y_0 > 0$ and the orbit of y_0 by H (resp. H^{-1}) tends monotonically to 0, then $I > 0$ (resp. $I < 0$) in the open interval $]0, y^*[$, for a small $y^* > 0$.

Theorem 3.1. *Consider a PWS slow-fast Liénard system (3) and assume that (4) is satisfied. Given $y_0 \in]0, y^*[$, let U be the orbit with the initial point y_0 (as defined above). Then $\dim_B U$ exists and*

$$\dim_B U \in \left\{ \frac{m-1}{m+1} \mid m = 1, 2, \dots \right\} \cup \{1\}. \quad (10)$$

If $\dim_B U \neq 0, 1$, then U is Minkowski nondegenerate. These results do not depend on the choice of the initial point $y_0 \in]0, y^[$.*

Remark 1. *From (10) in Theorem 3.1 it follows that $\dim_B U$ can take the following discrete set of values: $0, \frac{1}{3}, \frac{1}{2}, \frac{3}{5}, \frac{2}{3}, \frac{5}{7}, \dots, 1$. We point out that the values $\frac{1}{3}, \frac{3}{5}, \frac{5}{7}, \dots$ (m even) and 1 are found near smooth slow-fast Hopf points (see [7]). Besides these old values of the Minkowski dimension, the PWS slow-fast Hopf point in (3) also produces infinitely many new values: $0, \frac{1}{2}, \frac{2}{3}, \dots$ (m odd). See also Theorem 3.2 and Remark 2.*

The proof of Theorem 3.1 goes as follows (for more details we refer to Section 4.1). Firstly, using assumptions (4) we can write

$$F_{\pm}(x) = x^2 f_{\pm}(x),$$

where f_-, f_+ are C^∞ -smooth functions and $f_{\pm}(0) > 0$. Then, it can be easily checked that the homeomorphism

$$T(x, y) = \begin{cases} (x\sqrt{f_-(x)}, y), & x < 0, \\ (x, y), & x = 0, \\ (x\sqrt{f_+(x)}, y), & x > 0, \end{cases} \quad (11)$$

is a Σ -equivalence in the sense of [18, Definition 2.20], which brings X_- (resp. X_+) defined in (3), locally near $(x, y) = (0, 0)$, into \tilde{X}_- (resp. \tilde{X}_+), after multiplication by $\psi'_- > 0$ (resp. $\psi'_+ > 0$), where

$$\tilde{X}_- : \begin{cases} \dot{x} = y - x^2, \\ \dot{y} = \epsilon G_-(\psi_-(x))\psi'_-(x), \end{cases} \quad x \leq 0, \quad \tilde{X}_+ : \begin{cases} \dot{x} = y - x^2, \\ \dot{y} = \epsilon G_+(\psi_+(x))\psi'_+(x), \end{cases} \quad x \geq 0, \quad (12)$$

and ψ_{\pm} is the inverse of $x \rightarrow x\sqrt{f_{\pm}(x)}$. System (12) has a Liénard form similar to (3), with a PWS slow-fast Hopf point at $(x, y) = (0, 0)$. We show that (3) and (12) have the same slow relation function (Section 4.1), and therefore they produce the same orbits. Thus, it suffices to give a complete fractal classification of (12), using the Minkowski dimension. Such fractal classification is given in Theorem 3.2 below. In summary, Theorem 3.1 follows from Theorem 3.2.

We define

$$\bar{G}(x) := G_-(\psi_-(x))\psi'_-(x) + G_+(\psi_+(-x))\psi'_+(-x). \quad (13)$$

In what follows, $m_0(\bar{G})$ denotes the multiplicity of the zero $x = 0$ of \bar{G} , and $g_{m_0(\bar{G})} \neq 0$ denotes the $m_0(\bar{G})$ -th Taylor coefficient of \bar{G} about $x = 0$, if $m_0(\bar{G})$ is finite. In Section 4.1 we prove the following result.

Theorem 3.2. *Consider (12) and let H be its slow relation function. Given $y_0 \in]0, y^*[$, then the following statements hold.*

1. *Suppose that $1 \leq m_0(\bar{G}) < \infty$. If $(-1)^{m_0(\bar{G})+1}g_{m_0(\bar{G})} > 0$ (resp. < 0), then the orbit $U = \{y_l \mid l \in \mathbb{N}\}$ of y_0 by H (resp. H^{-1}) tends monotonically to 0 and holds the bijective correspondence*

$$m_0(\bar{G}) = \frac{1 + \dim_B U}{1 - \dim_B U}. \quad (14)$$

Moreover, if $1 < m_0(\bar{G}) < \infty$, then U is Minkowski nondegenerate.

2. *If $m_0(\bar{G}) = \infty$, then $\dim_B U = 1$.*

The above results do not depend on the choice of the initial point $y_0 \in]0, y^[$.*

Remark 2. *From (14), it follows that*

$$\dim_B U = \frac{m_0(\bar{G}) - 1}{m_0(\bar{G}) + 1}.$$

This and Statement 2 of Theorem 3.2 imply (10).

If we assume that F and G in (2) are C^∞ -smooth, then the function \bar{G} defined in (13) is even and, as a consequence of Theorem 3.2, we have the following sequence of values of $\dim_B U$: $1, \frac{1}{3}, \frac{3}{5}, \frac{5}{7}, \dots$

3.2 Fractal analysis of bounded balanced canard cycles

In this section we focus on the fractal analysis of bounded balanced canard cycles $\Gamma_{\hat{y}}$, with $\hat{y} > 0$. We call $\Gamma_{\hat{y}}$ a balanced canard cycle if $I(\hat{y}) = 0$, with I being the integral defined in (8). From now on, we assume that $\Gamma_{\hat{y}}$ is balanced. Due to Equations (6), (7) and the Implicit Function Theorem, it follows that there is a function $H(y)$ such that $H(\hat{y}) = \hat{y}$ and

$$I_-(H(y)) = I_+(y),$$

for y kept close to \hat{y} (see (9)). If we differentiate this last equation, we obtain $H' > 0$ (recall that $I'_\pm(y) < 0$). This implies that orbits generated by H are monotone.

Assume that there exists a small $y^* > 0$ such that I is nonzero in the open interval $]\hat{y}, \hat{y} + y^*[$. Given $y_0 \in]\hat{y}, \hat{y} + y^*[$, if $I > 0$ (resp. $I < 0$) in $]\hat{y}, \hat{y} + y^*[$, then U denotes the orbit $\{y_0, y_1, y_2, \dots\}$ defined by

$$I_-(y_{l+1}) = I_+(y_l) \quad (\text{resp. } I_-(y_l) = I_+(y_{l+1})), \quad \text{with } l \geq 0.$$

Notice that U is the orbit of y_0 by H (resp. H^{-1}) and it converges monotonically to \hat{y} as $l \rightarrow \infty$. See also Section 3.1.

Denote by $m_{\hat{y}}(I)$ the multiplicity of the zero $y = \hat{y}$ of I . When $m_{\hat{y}}(I)$ is finite, $i_{m_{\hat{y}}(I)} \neq 0$ is the $m_{\hat{y}}(I)$ -th Taylor coefficient of I about $y = \hat{y}$. The fractal classification of $\Gamma_{\hat{y}}$ is given in Theorem 3.3 and it will be proved in Section 4.2.

Theorem 3.3. *Consider system (3) and let H be its slow relation function defined near a balanced canard cycle $\Gamma_{\hat{y}}$. If $y_0 \in]\hat{y}, \hat{y} + y^*[$, then the following statements are true.*

1. *Suppose that $1 \leq m_{\hat{y}}(I) < \infty$. If $i_{m_{\hat{y}}(I)} > 0$ (resp. < 0), then the orbit $U = \{y_l \mid l \in \mathbb{N}\}$ of y_0 by H (resp. H^{-1}) tends monotonically to \hat{y} and the following bijective correspondence holds*

$$m_{\hat{y}}(I) = \frac{1}{1 - \dim_B U}. \quad (15)$$

Moreover, if $1 < m_{\hat{y}}(I) < \infty$, then U is Minkowski nondegenerate.

2. *If $m_{\hat{y}}(I) = \infty$, then $\dim_B U = 1$.*

The above results do not depend on the choice of the initial point $y_0 \in]\hat{y}, \hat{y} + y^[$.*

Remark 3. *Using (15), it follows that*

$$\dim_B U = \frac{m_{\hat{y}}(I) - 1}{m_{\hat{y}}(I)}.$$

This result, combined with Statement 2 of Theorem 3.3, produces the following set of values of $\dim_B U$: $0, \frac{1}{2}, \frac{2}{3}, \dots, 1$. We highlight that, in the PWS setting, we do not obtain new values of the Minkowski dimension in comparison with the smooth setting due to the C^∞ -smoothness of I_- and I_+ at $y = \hat{y}$. In other words, the above values also can be produced by balanced canard cycles in the smooth setting (see also [20]).

3.3 Fractal analysis of PWS classical Liénard equations near infinity

In this section we consider a special case of (3), namely PWS classical Liénard equations of degree $n + 1$, which are given by

$$\begin{cases} \dot{x} = y - \sum_{k=2}^{n+1} B_k^- x^k, & x \leq 0, \\ \dot{y} = -\epsilon A_1^- x, \end{cases} \quad \begin{cases} \dot{x} = y - \sum_{k=2}^{n+1} B_k^+ x^k, & x \geq 0, \\ \dot{y} = -\epsilon A_1^+ x, \end{cases} \quad (16)$$

where $n \in \mathbb{N}_1$, $B_{n+1}^\pm \neq 0$, $A_1^\pm > 0$ and $B_2^\pm > 0$. It is clear that system (16) satisfies (4). Additionally, it is assumed that (16) satisfies (6) with $L_- =]-\infty, 0[$ and $L_+ =]0, \infty[$. As a direct consequence of (6), we have $(-1)^{n+1} B_{n+1}^- > 0$ and $B_{n+1}^+ > 0$.

After a rescaling $(x, t) = (a^\pm X, c^\pm T)$, we can bring (16) into

$$\begin{cases} \dot{x} &= y - \left((-1)^{n+1} x^{n+1} + \sum_{k=2}^n b_k^- x^k \right) \\ \dot{y} &= -\epsilon a_1^- x \end{cases} \quad \begin{cases} \dot{x} &= y - \left(x^{n+1} + \sum_{k=2}^n b_k^+ x^k \right) \\ \dot{y} &= -\epsilon a_1^+ x \end{cases} \quad (17)$$

where $a_1^\pm > 0$, $b_2^\pm > 0$ (when $n = 1$, we have $b_2^\pm = 1$) and we denote (X, T) again by (x, t) . It can be easily checked that (16) and (17) have the same slow relation function, and therefore it suffices to give a complete fractal classification of (17) near infinity.

Denote $F_-(x) = (-1)^{n+1} x^{n+1} + \sum_{k=2}^n b_k^- x^k$, $F_+(x) = x^{n+1} + \sum_{k=2}^n b_k^+ x^k$ and $G_\pm(x) = -a_1^\pm x$. Then we have

$$\frac{F'_\pm(x)^2}{G_\pm(x)} = -\frac{(n+1)^2}{a_1^\pm} x^{2n-1} (1 + o(1)), \quad x \rightarrow \pm\infty.$$

This and (7) imply that $I_\pm(y) \rightarrow -\infty$ as $y \rightarrow +\infty$. Let us recall that I_\pm are (strictly) decreasing functions and $I_\pm(y) \rightarrow 0$ as y tends to 0. We conclude that the slow relation function H (see (9)) is well-defined for all $y > 0$.

We suppose that there exists $y^* > 0$ large enough such that $I = I_+ - I_-$ is nonzero in the open interval $]y^*, \infty[$. Given $y_0 \in]y^*, \infty[$, if $I < 0$ (resp. $I > 0$) on $]y^*, \infty[$, we define the orbit $U = \{y_0, y_1, y_2, \dots\}$ by

$$I_-(y_{l+1}) = I_+(y_l) \quad (\text{resp. } I_-(y_l) = I_+(y_{l+1})), \quad \text{with } l \geq 0.$$

Then U is the orbit of y_0 by H (resp. H^{-1}) and it tends monotonically to $+\infty$. We define the lower Minkowski dimension of U by

$$\underline{\dim}_B U = \underline{\dim}_B \left\{ \frac{1}{y_l^{\frac{1}{n+1}}} \mid l \in \mathbb{N} \right\}, \quad (18)$$

and similarly for the upper Minkowski dimension $\overline{\dim}_B U$. If $\underline{\dim}_B U = \overline{\dim}_B U$, then we denote it by $\dim_B U$ and call it the Minkowski dimension of U . In Section 4.3, system (17) will be studied on the Poincaré–Lyapunov disc of degree $(1, n+1)$ and the exponent of y_l in (18) is related to that degree (see also [8, Section 2] for more details).

We introduce the notation

$$\begin{aligned} F_+(x) - F_-(-x) &= \sum_{k=2}^n (b_k^+ + (-1)^{k+1} b_k^-) x^k \\ &= (b_2^+ - b_2^-) x^2 + (b_3^+ + b_3^-) x^3 + \dots + (b_n^+ + (-1)^{n+1} b_n^-) x^n \\ &=: f_2 x^2 + f_3 x^3 + \dots + f_n x^n. \end{aligned} \quad (19)$$

In the case $n = 1$, then $F_-(x) - F_+(-x) = 0$. When one of the coefficients f_k in (19) is nonzero, we denote by k_0 the maximal k with the property $f_k \neq 0$. Now we are able to state the main result of this section. Theorem 3.4 is proved in Section 4.3.

Theorem 3.4. *Consider system (17) and the associated slow relation function H . Given $y_0 \in]y^*, \infty[$, the following statements hold.*

1. Suppose that $a_1^- \neq a_1^+$. If $a_1^- > a_1^+$ (resp. $a_1^- < a_1^+$), then the orbit $U = \{y_l \mid l \in \mathbb{N}\}$ of y_0 by H (resp. H^{-1}) tends monotonically to $+\infty$ and

$$\dim_B U = 0.$$

2. Suppose that $a_1^- = a_1^+$ and that one of the coefficients f_k is nonzero with $k_0 \neq n - 1$. If $f_{k_0}(1 + k_0 - n) > 0$ (resp. $f_{k_0}(1 + k_0 - n) < 0$), then the orbit $U = \{y_l \mid l \in \mathbb{N}\}$ of y_0 by H (resp. H^{-1}) tends monotonically to $+\infty$, U is Minkowski nondegenerate and

$$\dim_B U = \frac{n + 1 - k_0}{n + 2 - k_0}. \quad (20)$$

These results do not depend on the choice of the initial point y_0 .

If $a_1^- = a_1^+$ and $f_2 = \dots = f_n = 0$, then we have $H(y) = y$ ($I \equiv 0$) and each orbit U is a fixed point of H with the trivial Minkowski dimension ($\dim_B U = 0$).

Remark 4. Suppose that $F_- = F_+$ and it is a polynomial of even degree $n + 1$ (n odd) and $G_- = G_+$ ($a_1^- = a_1^+$). Then (19) implies that $f_k = 0$ for k even (hence, k_0 is odd and $k_0 \neq n - 1$). From (20) it follows that we have the following Minkowski dimensions of U : $\frac{1}{2}, \frac{3}{4}, \dots, \frac{n-4}{n-3}, \frac{n-2}{n-1}$ (see also [8, Remark 1]).

In the PWS setting, we get for n odd or even: $0, \frac{1}{2}, \frac{3}{4}, \frac{4}{5}, \dots, \frac{n-2}{n-1}, \frac{n-1}{n}$. We refer to Statement 1 and Statement 2 of Theorem 3.4. The case $k_0 = n - 1$ is a topic of further study. We believe that in this case the Minkowski dimension is different from $\frac{2}{3}$ and we have to deal with more complicated expansions of functions.

4 Proof of Theorems 3.1–3.4

4.1 Proof of Theorems 3.1 and 3.2

We consider (3) and assume that (4) is satisfied. Recall that the integrals I_- and I_+ are defined in (7) and I in (8). We denote by $\tilde{I}_-, \tilde{I}_+, \tilde{I}$ the integrals I_-, I_+, I computed for system (12):

$$\tilde{I}_\pm(y) = -4 \int_{\pm\sqrt{y}}^0 \frac{x^2}{G_\pm(\psi_\pm(x))\psi'_\pm(x)} dx, \quad \tilde{I}(y) = \tilde{I}_+(y) - \tilde{I}_-(y). \quad (21)$$

Since the slow divergence integral is invariant under changes of coordinates and time reparameterizations (see [6, Chapter 5]), we have $\tilde{I}_\pm(y) = I_\pm(y)$ (this can be easily seen if we use the change of variable $s = \psi_\pm(x)$ in \tilde{I}_\pm). Now, it is clear that H defined in (9) is also the slow relation function of (12) ($\tilde{I}_-(H(y)) = \tilde{I}_+(y)$). This implies that Theorem 3.1 follows from Theorem 3.2. Therefore, in the rest of this section we prove Theorem 3.2 and, from now on, When we refer to (21), we use I_-, I_+, I instead of $\tilde{I}_-, \tilde{I}_+, \tilde{I}$.

We will prove Theorem 3.2 for $I > 0$ on $]0, y^*[$. Let $y_0 \in]0, y^*[$. Then the orbit U of y_0 by H tends monotonically to 0 as $l \rightarrow \infty$ ($I_-(y_{l+1}) = I_+(y_l)$ with $l \geq 0$, see Section 3.1). The case where $I < 0$ on $]0, y^*[$ can be treated in a similar fashion.

We introduce the notation

$$g_{\pm}(x) = G_{\pm}(\psi_{\pm}(x))\psi'_{\pm}(x),$$

and therefore Equation (13) can be written as

$$\bar{G}(x) = g_{-}(x) + g_{+}(-x).$$

From assumption (4) and the definition of ψ_{\pm} after (12), it follows that $g_{\pm}(0) = 0$ and $g'_{\pm}(0) < 0$. Moreover, using Taylor series of g_{\pm} at the origin, one can write the integrand in (21) as

$$\frac{x^2}{g_{\pm}(x)} = \frac{1}{g'_{\pm}(0)}x + O(x^2). \quad (22)$$

For the integral $I(y_l)$ we get

$$\begin{aligned} I(y_l) &= I_{+}(y_l) - I_{-}(y_{l+1}) + I_{-}(y_{l+1}) - I_{-}(y_l) \\ &= 4 \int_{-\sqrt{y_l}}^{-\sqrt{y_{l+1}}} \frac{x^2}{g_{-}(x)} dx \\ &= -\frac{2}{g'_{-}(0)} y_l \int_{\frac{y_{l+1}}{y_l}}^1 (1 + O(\sqrt{y_l s})) ds. \end{aligned} \quad (23)$$

In the second step in (23) we use $I_{-}(y_{l+1}) = I_{+}(y_l)$ and in the last step we use (22) and then the change of variable $s = \frac{x^2}{y_l}$.

The idea is to compare (23) with equivalent asymptotic expansions of (21). There are three cases that must be considered: $m_0(\bar{G}) = 1$, $1 < m_0(\bar{G}) < \infty$ and $m_0(\bar{G}) = \infty$.

(a) $m_0(\bar{G}) = 1$. This holds if, and only if, $g'_{-}(0) \neq g'_{+}(0)$.

Using (21) and (22), we get

$$\begin{aligned} I(y) &= -4 \int_{\sqrt{y}}^0 \frac{x^2}{g_{+}(x)} dx + 4 \int_{-\sqrt{y}}^0 \frac{x^2}{g_{-}(x)} dx \\ &= 2 \left(\frac{1}{g'_{+}(0)} - \frac{1}{g'_{-}(0)} \right) y(1 + o(1)), \end{aligned} \quad (24)$$

where $o(1)$ tends to zero as $y \rightarrow 0$. It is clear from (24) that $I > 0$ is equivalent to $g'_{-}(0) > g'_{+}(0)$ (and recall that $g'_{\pm}(0) < 0$). From (24) with $y = y_l$, (23) and $y_l \rightarrow 0$ as $l \rightarrow \infty$ it follows that

$$\lim_{l \rightarrow \infty} \frac{y_{l+1}}{y_l} = \frac{g'_{-}(0)}{g'_{+}(0)} \in]0, 1[.$$

This implies that the orbit U converges exponentially to zero as $l \rightarrow \infty$, that is, there exist $\lambda \in]0, 1[$ and a constant $c > 0$ such that $0 < y_l \leq c\lambda^l$ for all l . It follows from [12, Lemma 1] that $\dim_B U = 0$ and the Minkowski dimension does not depend on the choice of y_0 . This completes the proof of Statement 1 of Theorem 3.2 when $m_0(\bar{G}) = 1$.

(b) $1 < m_0(\bar{G}) < \infty$. This holds if, and only if, $g'_-(0) = g'_+(0)$. Using Taylor series at 0, one can write the integrand of (21) as

$$\begin{aligned} \frac{x^2}{g_{\pm}(x)} &= \frac{x^2}{T_{\pm}(x) + \gamma_{\pm}x^{m_0(\bar{G})} + O(x^{m_0(\bar{G})+1})} \\ &= \frac{x^2}{T_{\pm}(x)} - \frac{\gamma_{\pm}}{(g'_{\pm}(0))^2}x^{m_0(\bar{G})} + O(x^{m_0(\bar{G})+1}), \end{aligned} \quad (25)$$

where T_{\pm} is the Taylor polynomial of degree $m_0(\bar{G}) - 1$ of g_{\pm} at $x = 0$, $T'_{\pm}(0) = g'_{\pm}(0)$ and γ_{\pm} is the $m_0(\bar{G})$ -th Taylor coefficient of g_{\pm} about $x = 0$. Notice that

$$g_{m_0(\bar{G})} = \gamma_- + (-1)^{m_0(\bar{G})}\gamma_+ \neq 0, \quad (26)$$

where $g_{m_0(\bar{G})}$ denotes the $m_0(\bar{G})$ -th Taylor coefficient of \bar{G} about $x = 0$ (recall its definition after Equation (13)). A direct consequence of (26) is

$$(-1)^{m_0(\bar{G})+1}g_{m_0(\bar{G})} = (-1)^{m_0(\bar{G})+1}\gamma_- - \gamma_+. \quad (27)$$

The integral I can be written as

$$\begin{aligned} I(y) &= -4 \int_{\sqrt{y}}^0 \frac{x^2}{T_+(x)} dx + 4 \int_{-\sqrt{y}}^0 \frac{x^2}{T_-(x)} dx \\ &\quad + \frac{4(-1)^{m_0(\bar{G})+1}g_{m_0(\bar{G})}}{(g'_+(0))^2(m_0(\bar{G})+1)} y^{\frac{m_0(\bar{G})+1}{2}} (1 + o(1)) \\ &= \frac{4(-1)^{m_0(\bar{G})+1}g_{m_0(\bar{G})}}{(g'_+(0))^2(m_0(\bar{G})+1)} y^{\frac{m_0(\bar{G})+1}{2}} (1 + o(1)), \end{aligned} \quad (28)$$

where $o(1)$ tends to zero as $y \rightarrow 0$. In the first step in (28) we use (21), (25), (26) and the fact that $g'_-(0) = g'_+(0)$ (because $m_0(\bar{G}) > 1$). We also used the relation (27). Moreover, in the second step we use the fact that

$$\int_{\sqrt{y}}^0 \frac{x^2}{T_+(x)} dx = \int_{-\sqrt{y}}^0 \frac{x^2}{T_-(x)} dx.$$

This follows directly from $T_-(x) = -T_+(-x)$ (observe that the Taylor polynomial $T_-(x) + T_+(-x)$ of degree $m_0(\bar{G}) - 1$ of \bar{G} , defined in (13), at $x = 0$ is identically zero). A simple consequence of (28) is that $I > 0$ if, and only if, $(-1)^{m_0(\bar{G})+1}g_{m_0(\bar{G})} > 0$.

Finally, (28) and The Mean Value Theorem for Integrals applied to (23) yield

$$y_l - y_{l+1} \simeq y_l^{\frac{m_0(\bar{G})+1}{2}}, l \rightarrow \infty, \quad (29)$$

where the notation \simeq was introduced in Section 2. Note that $\nu := \frac{m_0(\bar{G})+1}{2} > 1$. It follows from Equation (29) and [12, Theorem 1 and Remark 1] that the orbit U is Minkowski nondegenerate and

$$\dim_B U = 1 - \frac{1}{\nu} = \frac{m_0(\bar{G}) - 1}{m_0(\bar{G}) + 1},$$

and these results are independent of the choice of y_0 . We have proved Statement 1 of Theorem 3.2 for $1 < m_0(\bar{G}) < \infty$.

(c) $m_0(\bar{G}) = \infty$. Using similar steps to the ones used in case (b), it is not difficult to see that for every $\tilde{\nu} > 0$ then $I(y) = O(y^{\tilde{\nu}})$, when $y \rightarrow 0$. This and (23) imply that for every $\tilde{\nu} > 0$ then $y_l - y_{l+1} = O(y_l^{\tilde{\nu}})$, when $l \rightarrow \infty$. Following [12, Theorem 6] we have $\dim_B U = 1$, and once again the Minkowski dimension does not depend on y_0 . This completes the proof of Statement 2 of Theorem 3.2.

4.2 Proof of Theorem 3.3

Suppose that $\Gamma_{\hat{y}}$ is a balanced canard cycle with the associated slow relation function H defined in Section 3.2. We prove Theorem 3.3 for $I > 0$ in the open interval $]\hat{y}, \hat{y} + y^*[$. In this case, the orbit U of $y_0 \in]\hat{y}, \hat{y} + y^*[$ by H converges monotonically to \hat{y} as $l \rightarrow \infty$. We have $\hat{y} < H(y) < y$, for each $y \in]\hat{y}, \hat{y} + y^*[$. The case $I < 0$ on $]\hat{y}, \hat{y} + y^*[$ can be treated in a similar way.

We have

$$\begin{aligned} I(y) &= I_+(y) - I_-(y) \\ &= I_+(y) - I_-(H(y)) + I_-(H(y)) - I_-(y) \\ &= \int_{\alpha(y)}^{\alpha(H(y))} \frac{F'_-(x)^2}{G_-(x)} dx. \end{aligned}$$

In the last step, we use $I_-(H(y)) = I_+(y)$ and (7). From (6) and The Fundamental Theorem of Calculus, it follows that $\alpha'(y) < 0$ and

$$I(y) = \zeta(y)(y - H(y)),$$

where y is kept near \hat{y} and ζ is a positive smooth function. This implies that $y = \hat{y}$ is a zero of multiplicity m of $I(y)$ if, and only if, $y = \hat{y}$ is a zero of multiplicity m of $y - H(y)$.

We know that the following result holds (see [12, 32]).

Theorem 4.1. *Let \tilde{F} be a smooth function on $[0, \tilde{y}[$, $\tilde{F}(0) = 0$ and $0 < \tilde{F}(y) < y$ for each $y \in]0, \tilde{y}[$. Define $\tilde{H} = id - \tilde{F}$ and let U be the orbit of $y_0 \in]0, \tilde{y}[$ by \tilde{H} . Then $\dim_B U$ is independent of the initial point y_0 and, for $1 \leq m \leq \infty$, the following bijective correspondence holds:*

$$m = \frac{1}{1 - \dim_B U}$$

where m is the multiplicity of the zero $y = 0$ of \tilde{F} . If $m = \infty$, then $\dim_B U = 1$.

Theorem 3.3 follows from Theorem 4.1 with $\tilde{y} = y^*$, $\tilde{F}(y) = y + \hat{y} - H(y + \hat{y})$ and $\tilde{H}(y) = H(y + \hat{y}) - \hat{y}$. When $1 \leq m_{\hat{y}}(I) < \infty$, it is clear that $I > 0$ if, and only if $i_{m_{\hat{y}}(I)} > 0$. Moreover, for $1 < m_{\hat{y}}(I) < \infty$, the orbit U is Minkowski nondegenerate (see e.g. [12, Theorem 1]).

4.3 Proof of Theorem 3.4

In this section we focus on system (17) and prove Theorem 3.4. In Section 4.3.1, we study the Poincaré–Lyapunov compactification of (17) and detect the unbounded canard cycle. Section 4.3.2 is devoted to a fractal classification of (17) at infinity in the positive y -direction. In Section 4.3.3, we complete the proof of Theorem 3.4 by using the invariance of the slow divergence integral under changes of coordinates and changes of time.

4.3.1 Poincaré–Lyapunov compactification

This section is devoted to study the dynamics of (17) near infinity on the Poincaré–Lyapunov disc of degree $(1, n + 1)$.

In the positive x -direction we use the transformation

$$x = \frac{1}{r}, \quad y = \frac{\bar{y}}{r^{n+1}},$$

with $r > 0$ small and \bar{y} kept in a large compact set. In the new coordinates (r, \bar{y}) , system (17) becomes (after multiplication by r^n)

$$\begin{cases} \dot{r} &= -r \left(\bar{y} - 1 - \sum_{k=2}^n b_k^+ r^{n+1-k} \right), \\ \dot{\bar{y}} &= -\epsilon a_1^+ r^{2n} - (n+1)\bar{y} \left(\bar{y} - 1 - \sum_{k=2}^n b_k^+ r^{n+1-k} \right). \end{cases} \quad (30)$$

Suppose that $\epsilon = 0$. On the line $\{r = 0\}$ system (30) has two singular points: $\bar{y} = 0$ and $\bar{y} = 1$. The eigenvalues of the linear part at $\bar{y} = 0$ are given by $(1, n + 1)$ and the eigenvalues of $\bar{y} = 1$ are given by $(0, -(n + 1))$. This implies that $\bar{y} = 0$ is a hyperbolic repelling node and $\bar{y} = 1$ is a semi-hyperbolic singularity with the \bar{y} -axis as the stable manifold and the curve of singular points $\bar{y} = 1 + \sum_{k=2}^n b_k^+ r^{n+1-k}$ as center manifold.

It is not difficult to see, using the invariance under the flow and asymptotic expansions in ϵ , that center manifolds of (30) at $(r, \bar{y}, \epsilon) = (0, 1, 0)$ are given by

$$\bar{y} = 1 + \sum_{k=2}^n b_k^+ r^{n+1-k} - r^{2n} \left(\frac{a_1^+}{n+1} + O(r) \right) \epsilon + O(\epsilon^2).$$

If we substitute this for \bar{y} in the first component of (30), divide out ϵ and let $\epsilon \rightarrow 0$, we obtain the slow dynamics

$$r' = r^{2n+1} \left(\frac{a_1^+}{n+1} + O(r) \right).$$

Since $a_1^+ > 0$, the slow dynamics points away from the singularity $r = 0$.

In the negative x -direction we use the transformation

$$x = \frac{-1}{r}, \quad y = \frac{\bar{y}}{r^{n+1}},$$

and system (17) changes (after multiplication by r^n) into

$$\begin{cases} \dot{r} &= r \left(\bar{y} - 1 - \sum_{k=2}^n b_k^- (-1)^k r^{n+1-k} \right), \\ \dot{\bar{y}} &= \epsilon a_1^- r^{2n} + (n+1)\bar{y} \left(\bar{y} - 1 - \sum_{k=2}^n b_k^- (-1)^k r^{n+1-k} \right). \end{cases} \quad (31)$$

When $\epsilon = 0$, the line $\{r = 0\}$ contains two singularities of (31): $\bar{y} = 0$ and $\bar{y} = 1$. The eigenvalues of the linear part at $\bar{y} = 0$ (resp. $\bar{y} = 1$) are $(-1, -(n+1))$ (resp. $(0, n+1)$). Hence, $\bar{y} = 0$ is a hyperbolic attracting node and $\bar{y} = 1$ is a semi-hyperbolic singularity with the \bar{y} -axis as the unstable manifold. The curve of singularities is given by $\bar{y} = 1 + \sum_{k=2}^n b_k^- (-1)^k r^{n+1-k}$. The slow dynamics along the curve of singularities is given by

$$r' = r^{2n+1} \left(\frac{-a_1^-}{n+1} + O(r) \right),$$

and it points towards the origin $r = 0$ because $a_1^- > 0$.

In the positive and negative y -direction, there are no extra singularities. After putting all the information together, we get the phase portrait near infinity of (17) for $\epsilon = 0$, including direction of the slow dynamics (see Figure 3). Now, it is clear that the unbounded canard cycle consists of the curve of singularities of (17), denoted by S , and the regular orbit connecting the two semi-hyperbolic singularities at infinity (these two points are the end points of S).

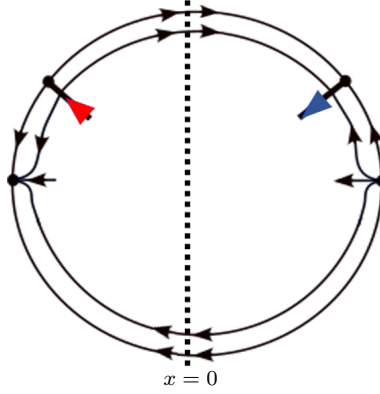


Figure 3: The phase portrait near infinity of (17), with $\epsilon = 0$. We have a crossing near the switching line $x = 0$.

4.3.2 Fractal Analysis Near Infinity

Since the attracting branch and the repelling branch of the curve of singularities are visible in the positive y -direction (see Figure 3), it is natural to present the fractal analysis in the positive y -direction. We have

$$x = \frac{\bar{x}}{r}, \quad y = \frac{1}{r^{n+1}},$$

and system (17) becomes (after multiplication by r^n)

$$\begin{cases} \dot{r} = \frac{\epsilon a_1^-}{n+1} r^{2n+1} \bar{x}, \\ \dot{\bar{x}} = 1 - \left((-1)^{n+1} \bar{x}^{n+1} + \sum_{k=2}^n b_k^- r^{n+1-k} \bar{x}^k \right) + \frac{\epsilon a_1^-}{n+1} r^{2n} \bar{x}^2, \quad \bar{x} \leq 0, \end{cases} \quad (32)$$

$$\begin{cases} \dot{r} = \frac{\epsilon a_1^+}{n+1} r^{2n+1} \bar{x}, \\ \dot{\bar{x}} = 1 - \left(\bar{x}^{n+1} + \sum_{k=2}^n b_k^+ r^{n+1-k} \bar{x}^k \right) + \frac{\epsilon a_1^+}{n+1} r^{2n} \bar{x}^2, \end{cases} \quad \bar{x} \geq 0. \quad (33)$$

When $\epsilon = 0$, system (32) has a normally repelling curve of singularities $\bar{x} = \Phi_-(r)$ satisfying $\Phi_-(0) = -1$ and

$$1 - (-1)^{n+1} \Phi_-(r)^{n+1} - \sum_{k=2}^n b_k^- r^{n+1-k} \Phi_-(r)^k = 0, \quad (34)$$

and (33) has a normally attracting curve of singularities $\bar{x} = \Phi_+(r)$ satisfying $\Phi_+(0) = 1$ and

$$1 - \Phi_+(r)^{n+1} - \sum_{k=2}^n b_k^+ r^{n+1-k} \Phi_+(r)^k = 0. \quad (35)$$

Recall from Equation (19) that $f_k = b_k^+ + (-1)^{k+1} b_k^-$, for $k = 2, \dots, n$. The following lemma gives a useful connection between Φ_- and Φ_+ .

Lemma 4.2. *The functions $\Phi_-(r)$ and $\Phi_+(r)$ defined in (34) (resp. (35)) satisfy*

$$\Phi_+(r) = -\Phi_-(r) - \frac{1}{n+1} \sum_{k=2}^n f_k r^{n+1-k} (1 + O(r)),$$

Proof. The lemma can be easily proved using $\Phi_+(r) = -\Phi_-(r)$ when $f_2 = \dots = f_n = 0$ (see (34) and (35)). \square

If we substitute $\Phi_-(r)$ (resp. $\Phi_+(r)$) for \bar{x} in the r -component of (32) (resp. (33)) and divide out ϵ , then we obtain the slow dynamics along $\bar{x} = \Phi_{\pm}(r)$:

$$r' = \frac{a_1^{\pm}}{n+1} r^{2n+1} \Phi_{\pm}(r). \quad (36)$$

Let $\tilde{r} > 0$ be small and fixed. For $r \in]0, \tilde{r}[$, we define the slow divergence integral of (32) along the portion $[r, \tilde{r}]$ of $\bar{x} = \Phi_-(r)$

$$J_-(r) = -(n+1) \int_r^{\tilde{r}} \frac{(n+1)(-1)^{n+1} \Phi_-(s)^n + \sum_{k=2}^n k b_k^- s^{n+1-k} \Phi_-(s)^{k-1}}{a_1^- s^{2n+1} \Phi_-(s)} ds < 0, \quad (37)$$

and the slow divergence integral of (33) along the portion $[r, \tilde{r}]$ of $\bar{x} = \Phi_+(r)$

$$J_+(r) = -(n+1) \int_r^{\tilde{r}} \frac{(n+1) \Phi_+(s)^n + \sum_{k=2}^n k b_k^+ s^{n+1-k} \Phi_+(s)^{k-1}}{a_1^+ s^{2n+1} \Phi_+(s)} ds < 0. \quad (38)$$

Observe that J_+ is the integral of the divergence of (33) for $\epsilon = 0$, computed in singular points $(s, \Phi_+(s))$, where the variable of integration is the time variable of the slow dynamics (36). A similar remark holds for the integral J_- (but it is computed in backward time). From (37) and (38) it follows that $J_{\pm}(r) \rightarrow -\infty$ as $r \rightarrow 0$.

Let $\tilde{J} \in \mathbb{R}$ be arbitrary but fixed. For $r_0 \in]0, \tilde{r}[$, we suppose that the sequence $(r_l)_{l \in \mathbb{N}}$, defined by

$$J_+(r_l) - J_-(r_{l+1}) = \tilde{J}, \quad l \geq 0,$$

tends monotonically to 0 as $l \rightarrow \infty$. The case where $(r_l)_{l \in \mathbb{N}}$, tending to 0 as $l \rightarrow \infty$, is defined by $J_+(r_{l+1}) - J_-(r_l) = \tilde{J}$ can be treated in a similar way.

Remark 5. In Section 4.3.3 the constant \tilde{J} will be equal to the slow divergence integral $-I\left(\frac{1}{\tilde{r}^{n+1}}\right)$, with I defined in (8).

We can write

$$J_+(r_l) - J_-(r_l) = \tilde{J} + J_-(r_{l+1}) - J_-(r_l). \quad (39)$$

Let us first study $J_+(r_l) - J_-(r_l)$. For simplicity sake, we write $\Phi_{\pm} = \Phi_{\pm}(s)$. From Lemma 4.2 and the relation $b_k^+ = f_k + (-1)^k b_k^-$, one can check that

$$\begin{aligned} & \frac{(n+1)\Phi_+^n + \sum_{k=2}^n k b_k^+ s^{n+1-k} \Phi_+^{k-1}}{a_1^+ \Phi_+} \\ &= \frac{(n+1)(-\Phi_-)^n + \sum_{k=2}^n k b_k^+ s^{n+1-k} (-\Phi_-)^{k-1}}{-a_1^+ \Phi_-} - \sum_{k=2}^n f_k s^{n+1-k} \left(\frac{n-1}{a_1^+} + O(s) \right) \\ &= \frac{-(n+1)(-1)^{n+1} \Phi_-^n - \sum_{k=2}^n k b_k^- s^{n+1-k} \Phi_-^{k-1} + \sum_{k=2}^n k f_k s^{n+1-k} (-\Phi_-)^{k-1}}{-a_1^- \Phi_- + (a_1^- - a_1^+) \Phi_-} \\ &\quad - \sum_{k=2}^n f_k s^{n+1-k} \left(\frac{n-1}{a_1^+} + O(s) \right) \\ &= \frac{(n+1)(-1)^{n+1} \Phi_-^n + \sum_{k=2}^n k b_k^- s^{n+1-k} \Phi_-^{k-1}}{a_1^- \Phi_-} \\ &\quad - \sum_{k=2}^n f_k s^{n+1-k} \left(\frac{n-1-k}{a_1^+} + O(s) \right) + (a_1^- - a_1^+) \left(\frac{n+1}{a_1^- a_1^+} + O(s) \right). \quad (40) \end{aligned}$$

Using the integrals (37), (38) and considering the integrand (40), it follows that

$$\begin{aligned} J_+(r_l) - J_-(r_l) &= (n+1) \int_{r_l}^{\tilde{r}} \frac{1}{s^{2n+1}} \sum_{k=2}^n f_k s^{n+1-k} \left(\frac{n-1-k}{a_1^+} + O(s) \right) ds \\ &\quad - (n+1) \int_{r_l}^{\tilde{r}} \frac{1}{s^{2n+1}} (a_1^- - a_1^+) \left(\frac{n+1}{a_1^- a_1^+} + O(s) \right) ds \\ &= \sum_{k=2}^n f_k r_l^{1-n-k} \left(\frac{(n+1)(1+k-n)}{a_1^+(1-n-k)} + o(1) \right) \\ &\quad + (a_1^- - a_1^+) r_l^{-2n} \left(-\frac{(n+1)^2}{2n a_1^- a_1^+} + o(1) \right) + \hat{J}, \quad (41) \end{aligned}$$

where $o(1) \rightarrow 0$ as $r_l \rightarrow 0$ and \hat{J} is a constant independent of r_l .

Now, consider the term $J_-(r_{l+1}) - J_-(r_l)$ in (39). Using (37), we have

$$\begin{aligned} J_-(r_{l+1}) - J_-(r_l) &= -\frac{(n+1)^2}{a_1^-} \int_{r_{l+1}}^{r_l} \frac{1}{s^{2n+1}} (1 + O(s)) ds \\ &= -\frac{(n+1)^2}{a_1^- r_l^{2n}} \int_{\frac{r_{l+1}}{r_l}}^1 \frac{1}{\tilde{s}^{2n+1}} (1 + O(r_l \tilde{s})) d\tilde{s}, \end{aligned} \quad (42)$$

where in the last step we use the change of variable $s = r_l \tilde{s}$.

Now, we use (41) and (42) in the Equation (39) and then we get

$$\begin{aligned} &-\frac{(n+1)^2}{a_1^-} \int_{\frac{r_{l+1}}{r_l}}^1 \frac{1}{\tilde{s}^{2n+1}} (1 + O(r_l \tilde{s})) d\tilde{s} \\ &= \sum_{k=2}^n f_k r_l^{n+1-k} \left(\frac{(n+1)(1+k-n)}{a_1^+(1-n-k)} + o(1) \right) \\ &\quad + (a_1^- - a_1^+) \left(-\frac{(n+1)^2}{2na_1^- a_1^+} + o(1) \right) + r_l^{2n} (\hat{J} - \tilde{J}). \end{aligned} \quad (43)$$

We distinguish between two cases: $a_1^- \neq a_1^+$ and $a_1^- = a_1^+$. Recall that $a_1^\pm > 0$.

Case $a_1^- \neq a_1^+$. Since $(r_l)_{l \in \mathbb{N}}$ tends monotonically to 0 as $l \rightarrow \infty$, it can be easily seen that (43) implies

$$\lim_{l \rightarrow \infty} \frac{r_{l+1}}{r_l} = \left(\frac{a_1^+}{a_1^-} \right)^{\frac{1}{2n}} \in]0, 1[.$$

Since $a_1^- > a_1^+$, we conclude that $\dim_B(r_l)_{l \in \mathbb{N}} = 0$ and the Minkowski dimension does not depend on the choice of the initial point $r_0 \in]0, \tilde{r}[$ (see Section 4.1). We remark that when the sequence $(r_l)_{l \in \mathbb{N}}$, converging monotonically to 0 as $l \rightarrow \infty$, is defined by $J_+(r_{l+1}) - J_-(r_l) = \tilde{J}$, we have $a_1^- < a_1^+$.

Case $a_1^- = a_1^+$. Now the right-hand side of (43) tends to 0 as $l \rightarrow \infty$, and we get

$$\lim_{l \rightarrow \infty} \frac{r_{l+1}}{r_l} = 1. \quad (44)$$

Suppose that one of the coefficients f_k is nonzero. Then k_0 is well-defined (see Section 3.3) and from (43) it follows that

$$\int_{\frac{r_{l+1}}{r_l}}^1 \frac{1}{\tilde{s}^{2n+1}} (1 + O(r_l \tilde{s})) d\tilde{s} = f_{k_0} r_l^{n+1-k_0} \left(\frac{1+k_0-n}{(n+k_0-1)(n+1)} + o(1) \right), \quad (45)$$

where $o(1) \rightarrow 0$ as $r_l \rightarrow 0$.

Notice that

$$\kappa \leq \frac{1}{\tilde{s}^{2n+1}} (1 + O(r_l \tilde{s})) \leq \frac{1}{\kappa} \left(\frac{r_l}{r_{l+1}} \right)^{2n+1}, \quad \forall \tilde{s} \in \left[\frac{r_{l+1}}{r_l}, 1 \right],$$

for $\kappa > 0$ small enough. This, (44) and (45) imply

$$r_l - r_{l+1} \simeq r_l^{n+2-k_0}, \quad l \rightarrow \infty,$$

if $f_{k_0}(1+k_0-n) > 0$. The notation \simeq was introduced in Section 2. As $n+2-k_0 > 1$ (recall that $k_0 \leq n$), we have that $(r_l)_{l \in \mathbb{N}}$ is Minkowski nondegenerate,

$$\dim_B(r_l)_{l \in \mathbb{N}} = 1 - \frac{1}{n+2-k_0} = \frac{n+1-k_0}{n+2-k_0}, \quad (46)$$

and this is independent of the choice of $r_0 \in]0, \tilde{r}[$ (see Section 4.1).

When $(r_l)_{l \in \mathbb{N}}$, tending (monotonically) to 0 as $l \rightarrow \infty$, is defined by $J_+(r_{l+1}) - J_-(r_l) = \tilde{J}$, we assume $f_{k_0}(1+k_0-n) < 0$.

4.3.3 Completing the proof of Theorem 3.4

Using $x = \frac{\tilde{x}}{r}$, $y = \frac{1}{r^{n+1}}$ we have the following relation between F_{\pm} , defined in Section 3.3, and Φ_{\pm} satisfying (34) and (35):

$$\frac{1}{r^{n+1}} = F_{\pm} \left(\frac{\Phi_{\pm}(r)}{r} \right). \quad (47)$$

The invariance of the slow divergence integral under changes of coordinates and time reparameterizations implies that

$$J_{\pm}(r) = - \int_{\frac{\Phi_{\pm}(r)}{r}}^{\frac{\Phi_{\pm}(\tilde{r})}{\tilde{r}}} \frac{F'_{\pm}(x)^2}{G_{\pm}(x)} dx, \quad \forall r \in]0, \tilde{r}[, \quad (48)$$

with J_{\pm} defined in (37) and (38) and $G_{\pm}(x) = -a_{\mp}^{\pm} x$ (we use the change of variable $x = \frac{\Phi_{\pm}(s)}{s}$).

Assume that $I = I_+ - I_-$ defined in (8) is negative on $]y^*, \infty[$, where $y^* > 0$ is large enough, and let $y_0 \in]y^*, \infty[$. (We take \tilde{r} such that $y^* = \frac{1}{\tilde{r}^{n+1}}$.) Then the orbit $U = \{y_0, y_1, y_2, \dots\}$ generated by $I_-(y_{l+1}) = I_+(y_l)$, $l \geq 0$, tends monotonically to $+\infty$ (see Section 3.3). If we write $r_l := \frac{1}{y_l^{n+1}}$ (see (18)), then it is clear that $(r_l)_{l \in \mathbb{N}}$ tends monotonically to 0, and

$$\begin{aligned} I_+(y_l) - I_-(y_{l+1}) &= I_+ \left(\frac{1}{r_l^{n+1}} \right) - I_- \left(\frac{1}{r_{l+1}^{n+1}} \right) \\ &= - \int_{\frac{\Phi_+(r_l)}{r_l}}^0 \frac{F'_+(x)^2}{G_+(x)} dx + \int_{\frac{\Phi_-(r_{l+1})}{r_{l+1}}}^0 \frac{F'_-(x)^2}{G_-(x)} dx \\ &= J_+(r_l) - \int_{\frac{\Phi_+(\tilde{r})}{\tilde{r}}}^0 \frac{F'_+(x)^2}{G_+(x)} dx - J_-(r_{l+1}) + \int_{\frac{\Phi_-(\tilde{r})}{\tilde{r}}}^0 \frac{F'_-(x)^2}{G_-(x)} dx \\ &= J_+(r_l) - J_-(r_{l+1}) + I \left(\frac{1}{\tilde{r}^{n+1}} \right) \end{aligned}$$

where we use (47) and (48). This implies that $(r_l)_{l \in \mathbb{N}}$ is generated by $J_+(r_l) - J_-(r_{l+1}) = \tilde{J}$, where $\tilde{J} := -I \left(\frac{1}{\tilde{r}^{n+1}} \right)$ and we can therefore use the results of Section 4.3.2. Statement 1 (resp. Statement 2) of Theorem 3.4 follows from (18) and the case $a_{\mp}^- \neq a_{\mp}^+$ (resp. $a_{\mp}^- = a_{\mp}^+$) in Section 4.3.2. (If I is positive on $]y^*, \infty[$, then we use $I_-(y_l) = I_+(y_{l+1})$ and $J_+(r_{l+1}) - J_-(r_l) = \tilde{J}$.) This completes the proof of Theorem 3.4.

5 Crossing limit cycles and Minkowski dimension

In this section we consider the piecewise smooth system of Liénard equations

$$\begin{cases} \dot{x} = y - F_-(x), \\ \dot{y} = \epsilon^2(\epsilon\alpha_- + G_-(x)), \end{cases} \quad x \leq 0, \quad \begin{cases} \dot{x} = y - F_+(x), \\ \dot{y} = \epsilon^2(\epsilon\alpha_+ + G_+(x)), \end{cases} \quad x \geq 0, \quad (49)$$

where $0 < \epsilon \ll 1$, α_{\pm} are regular parameters kept near 0 and C^{∞} -smooth functions F_{\pm} and G_{\pm} satisfy (4) (see Section 3). We define

$$\beta_{\pm} := -\frac{2G'_{\pm}(0)}{F''_{\pm}(0)} > 0. \quad (50)$$

A natural question that arises is how to link the Minkowski dimension of orbits defined in Sections 3.1 to 3.3 with the number of crossing limit cycles that (49) can have for $\epsilon > 0$. If the Minkowski dimension of orbits tending monotonically to $y = 0$ is trivial or, equivalently, $\beta_- \neq \beta_+$ (see Theorem 3.2 and note that $\beta_- \neq \beta_+$ if, and only if, $m_0(\bar{G}) = 1$), then there are no limit cycles near the PWS Hopf point (for the precise statement see Proposition 5.2 in Section 5.1). The condition $\beta_- \neq \beta_+$ means that, after blowing-up the vector field (49) $+ 0 \frac{\partial}{\partial \epsilon}$, the connection on the blow-up locus between the attracting branch $\{y = F_+(x)\}$ and the repelling branch $\{y = F_-(x)\}$ does not exist (see Figure 4).

In Section 5.2 we show that trivial Minkowski dimension of orbits tending monotonically to a balanced bounded canard cycle (see Section 3.2) is not equivalent to $\beta_- \neq \beta_+$. Indeed, we find a system (49) undergoing a saddle-node bifurcation of limit cycles and a system without limit cycles in which, in both cases, the Minkowski dimension is trivial. Finally, in Section 5.3 we provide examples of PWS classical Liénard equations (49) such that the Minkowski dimension of the unbounded canard cycle Γ_{∞} is trivial.

It is convenient to set ϵ^2 in (49) instead of ϵ when we introduce a family blow-up at the PWS Hopf point (see Section 5.1).

5.1 Limit cycles near the PWS Hopf point

Our goal is to study limit cycles of (49) in a small ϵ -uniform neighborhood of the origin $(x, y) = (0, 0)$ (i.e., the neighborhood does not shrink to the origin as $\epsilon \rightarrow 0$). For this purpose, we start our analysis by performing a blow-up transformation

$$(x, y, \epsilon) = (\rho\bar{x}, \rho^2\bar{y}, \rho\bar{\epsilon}),$$

with $(\bar{x}, \bar{y}, \bar{\epsilon}) \in \mathbb{S}^2$, $\rho \geq 0$ and $\bar{\epsilon} \geq 0$. We work with different charts. We point out that only the phase directional chart $\{\bar{y} = 1\}$ and the family chart $\{\bar{\epsilon} = 1\}$ are relevant for the study of limit cycles of (49), produced by the PWS Hopf point or (bounded and unbounded) canard cycles (see Figure 4).

5.1.1 Dynamics in the chart $\bar{y} = 1$

Using the coordinate change $(x, y, \epsilon) = (\rho\bar{x}, \rho^2, \rho\bar{\epsilon})$, with small $\rho \geq 0$ and $\epsilon \geq 0$ and \bar{x} kept in a large compact subset of \mathbb{R} , we obtain (after division by ρ)

$$\begin{cases} \dot{\bar{x}} &= 1 - \frac{F''_{\pm}(0)}{2}\bar{x}^2 + O(\rho\bar{x}^3) - \frac{1}{2}\bar{x}\bar{\epsilon}^2 (\bar{\epsilon}\alpha_{\pm} + G'_{\pm}(0)\bar{x} + O(\rho\bar{x}^2)), \\ \dot{\rho} &= \frac{1}{2}\rho\bar{\epsilon}^2 (\bar{\epsilon}\alpha_{\pm} + G'_{\pm}(0)\bar{x} + O(\rho\bar{x}^2)), \\ \dot{\bar{\epsilon}} &= -\frac{1}{2}\bar{\epsilon}^3 (\bar{\epsilon}\alpha_{\pm} + G'_{\pm}(0)\bar{x} + O(\rho\bar{x}^2)). \end{cases} \quad (51)$$

System (51) with $-$ (resp. $+$) is defined on $\bar{x} \leq 0$ (resp. $\bar{x} \geq 0$). Let us briefly describe the dynamics of (51). In the invariant line $\{\rho = \bar{\epsilon} = 0\}$ there are two singularities $\bar{x} = \pm\sqrt{\frac{2}{F''_{\pm}(0)}}$, which we will denote by p_{\pm} . Both singularities have two-dimensional center manifolds, and the unstable (resp. stable) manifold of p_{-} (resp. p_{+}) is the \bar{x} -axis. Such singularities correspond to the intersection of the critical manifold with the blow-up locus. The center behavior near p_{\pm} is given by

$$\begin{cases} \dot{\rho} &= \frac{1}{2}\rho\bar{\epsilon}^2 \left(\pm G'_{\pm}(0)\sqrt{\frac{2}{F''_{\pm}(0)}} + O(\rho, \bar{\epsilon}) \right), \\ \dot{\bar{\epsilon}} &= -\frac{1}{2}\bar{\epsilon}^3 \left(\pm G'_{\pm}(0)\sqrt{\frac{2}{F''_{\pm}(0)}} + O(\rho, \bar{\epsilon}) \right). \end{cases}$$

5.1.2 Dynamics in the chart $\bar{\epsilon} = 1$

Using the rescaling $(x, y) = (\epsilon\bar{x}, \epsilon^2\bar{y})$, with (\bar{x}, \bar{y}) kept in a large compact set, one obtains (after division by ϵ) the PWS system

$$\begin{cases} \dot{\bar{x}} &= \bar{y} - \frac{F''_{\pm}(0)}{2}\bar{x}^2 + O(\epsilon\bar{x}^3), \\ \dot{\bar{y}} &= \alpha_{\pm} + G'_{\pm}(0)\bar{x} + O(\epsilon\bar{x}^2), \end{cases} \quad \begin{cases} \dot{\bar{x}} &= \bar{y} - \frac{F''_{\pm}(0)}{2}\bar{x}^2 + O(\epsilon\bar{x}^3), \\ \dot{\bar{y}} &= \alpha_{\pm} + G'_{\pm}(0)\bar{x} + O(\epsilon\bar{x}^2). \end{cases} \quad (52)$$

Let us describe the dynamics in the top of the blow-up locus. For $\epsilon = 0$ and $\alpha_{\pm} = 0$, the PWS system (52) has the following form:

$$\begin{cases} \dot{\bar{x}} &= \bar{y} - \frac{F''_{\pm}(0)}{2}\bar{x}^2, & \bar{x} \leq 0, \\ \dot{\bar{y}} &= G'_{\pm}(0)\bar{x}, \end{cases} \quad \begin{cases} \dot{\bar{x}} &= \bar{y} - \frac{F''_{\pm}(0)}{2}\bar{x}^2, & \bar{x} \geq 0. \\ \dot{\bar{y}} &= G'_{\pm}(0)\bar{x}, \end{cases} \quad (53)$$

A first integral of (53) is given by

$$H_{\pm}(\bar{x}, \bar{y}) = e^{-\frac{2\bar{y}}{\beta_{\pm}}} \left(-\frac{\bar{y}}{\beta_{\pm}} + G'_{\pm}(0)\frac{\bar{x}^2}{\beta_{\pm}^2} + \frac{1}{2} \right),$$

where β_{\pm} were defined in (50). Note that p_{-} (resp. p_{+}) defined in Section 5.1.1 is the end point of the invariant curve $\{\bar{y} = -G'_{-}(0)\frac{\bar{x}^2}{\beta_{-}} - \frac{\beta_{-}}{2}, \bar{x} \leq 0\}$ (resp. $\{\bar{y} = -G'_{+}(0)\frac{\bar{x}^2}{\beta_{+}} - \frac{\beta_{+}}{2}, \bar{x} \geq 0\}$), corresponding to the level $H_{-}(\bar{x}, \bar{y}) = 0$ (resp. $H_{+}(\bar{x}, \bar{y}) = 0$). Moreover, the curve intersects the switching locus at $(0, -\frac{\beta_{-}}{2})$ (resp. $(0, -\frac{\beta_{+}}{2})$). The origin $(\bar{x}, \bar{y}) = (0, 0)$ is a center for both vector fields in (53) and it corresponds to the levels $H_{\pm}(\bar{x}, \bar{y}) = \frac{1}{2}$. The origin has a “focus-like” behavior for $\beta_{-} \neq \beta_{+}$ and a “center-like” behavior for $\beta_{-} = \beta_{+}$. See Figure 4.

It is now clear that, for $\beta_{-} = \beta_{+}$, the study of crossing limit cycles of (49) in a small ϵ -uniform neighborhood of the origin $(x, y) = (0, 0)$ has three

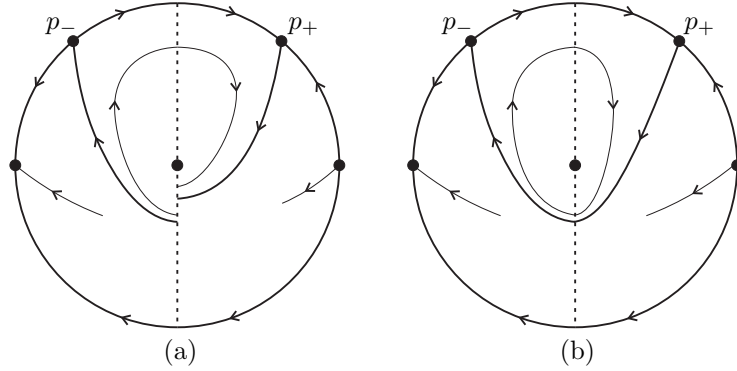


Figure 4: Phase portraits of the blown-up vector field (53) for $\beta_- \neq \beta_+$ (Figure (a)) and $\beta_- = \beta_+$ (Figure (b)). Each of the charts $\{\bar{x} = \pm 1\}$ contains one extra singularity of hyperbolic type. In the chart $\{\bar{y} = -1\}$ the dynamics is regular pointing from the right to the left.

components: (1) the study near the origin $(\bar{x}, \bar{y}) = (0, 0)$ inside the family (52), (2) the study near the singular polycycle (it consists of p_- and p_+ and the regular orbits that are heteroclinic to them), combining (51) and (52), and (3) the study near “ovals” surrounding the origin inside the family (52). This is a topic of further study.

Suppose that $\beta_- \neq \beta_+$. Then the connection between p_+ and p_- is broken (see Figure 4(a)). We consider the half return maps $\Pi_{\pm} :]0, \infty[\rightarrow]-\frac{\beta_{\pm}}{2}, 0[$. We define Π_+ by considering the flow of (53) in forward time and Π_- by considering the flow of (53) in backward time.

Proposition 5.1. *Consider system (53). If $\beta_- \neq \beta_+$, then the difference map $\Delta(\bar{y}) = \Pi_+(\bar{y}) - \Pi_-(\bar{y})$ does not have zeros in the interval $]0, \infty[$.*

Proof. For any $\bar{y} \in]0, \infty[$, the points $(0, \bar{y})$ and $(0, \Pi_{\pm}(\bar{y}))$ belong to the same level curve $H_{\pm}(\bar{x}, \bar{y}) = h_{\pm}$, with $0 < h_{\pm} < \frac{1}{2}$. If we write $H_{\pm}(\bar{y}) := H_{\pm}(0, \bar{y})$, then we have $H_{\pm}(\bar{y}) = H_{\pm}(\Pi_{\pm}(\bar{y}))$. This implies

$$H'_{\pm}(\bar{y}) = H'_{\pm}(\Pi_{\pm}(\bar{y}))\Pi'_{\pm}(\bar{y}). \quad (54)$$

From (54) it follows that $u = \Pi_{\pm}(\bar{y})$ is the $\bar{y} > 0$ -subset of the stable manifold of the hyperbolic saddle $(u, \bar{y}) = (0, 0)$ of

$$\begin{cases} \dot{u} &= \bar{y}e^{-\frac{2\bar{y}}{\beta_{\pm}}}, \\ \dot{\bar{y}} &= ue^{-\frac{2u}{\beta_{\pm}}}. \end{cases} \quad (55)$$

We remark that $u = \Pi_{\pm}(\bar{y})$ are contained in the second quadrant $\{u < 0, \bar{y} > 0\}$. The result follows by showing that $u = \Pi_-(\bar{y})$ and $u = \Pi_+(\bar{y})$ do not have intersection points in the second quadrant. Suppose by contradiction that they intersect in the second quadrant. This would imply the existence of contact points between the orbits of system (55) with β_- and the separatrix $u = \Pi_+(\bar{y})$. However, observe that

$$(\bar{y}e^{-\frac{2\bar{y}}{\beta_-}}, ue^{-\frac{2u}{\beta_-}}) \cdot (ue^{-\frac{2u}{\beta_+}}, -\bar{y}e^{-\frac{2\bar{y}}{\beta_+}}) = u\bar{y} \left(e^{-\frac{2\bar{y}}{\beta_-} - \frac{2u}{\beta_+}} - e^{-\frac{2\bar{y}}{\beta_+} - \frac{2u}{\beta_-}} \right).$$

For $\beta_- \neq \beta_+$, the last equation only vanishes in the set $\{u\bar{y}(u - \bar{y}) = 0\}$, and therefore there are no contact points in the second quadrant. \square

A direct consequence of Proposition 5.1 is the following.

Proposition 5.2. *Consider the PWS Liénard equation (49) with $\beta_- \neq \beta_+$. Let $[\bar{y}_1, \bar{y}_2] \subset]0, \infty[$. Then there exist $\epsilon_0 > 0$ and a small neighborhood \mathcal{U}_\pm of $\alpha_\pm = 0$ such that for each $(\epsilon, \alpha_-, \alpha_+) \in [0, \epsilon_0] \times \mathcal{U}_- \times \mathcal{U}_+$ the difference map $\Delta_{\epsilon, \alpha_-, \alpha_+}(\bar{y})$ associated to (52) does not have zeros in $[\bar{y}_1, \bar{y}_2]$.*

Observe that we do not study limit cycles bifurcating close to the origin of the phase space of (52).

5.2 Limit cycles near bounded canard cycles

Consider the PWS Liénard equation

$$\begin{cases} \dot{x} = y - \frac{x^2}{2}, \\ \dot{y} = \epsilon \left(-(1 + \delta)x - \frac{x^2}{2} + x^4 \right), \end{cases} \quad x \leq 0, \quad \begin{cases} \dot{x} = y - \frac{x^2}{2}, \\ \dot{y} = \epsilon \left(-x - \frac{x^2}{2} + x^4 \right), \end{cases} \quad x \geq 0, \quad (56)$$

with $\delta \in \mathbb{R}$ kept close to 0. This section is devoted to prove the following proposition.

Proposition 5.3. *There is a continuous function $\hat{y} :]-\delta_0, \delta_0[\rightarrow \mathbb{R}$ with $\delta_0 > 0$ small and satisfying $\hat{y}(0) > 0$ such that, for each $\delta \in]-\delta_0, \delta_0[$, $y = \hat{y}(\delta)$ is a simple zero of the slow divergence integral I_δ of (56), defined in (57).*

Concerning System (56), Proposition 5.3 and Theorem 3.3 (see also Remark 3) imply that, for each $\delta \in]-\delta_0, \delta_0[$, the Minkowski dimension of any entry-exit orbit tending monotonically to $\hat{y}(\delta)$ is equal to 0.

It can be checked that system (56) satisfies (4) for δ sufficiently small, and the curve of singularities is given by $S = \{y = \frac{x^2}{2}\}$. The associated slow dynamics is given by (see also (5))

$$x' = -1 - \delta - \frac{x}{2} + x^3, \text{ for } x \leq 0, \quad x' = -1 - \frac{x}{2} + x^3, \text{ for } x \geq 0.$$

The slow dynamics has a simple zero $x_0 > 0$ and it is strictly negative for all $x \in]-x_0, x_0[$ and δ small enough. One can compute x_0 numerically, and we obtain $x_0 \approx 1,16537$.

Using (8) we get

$$I_\delta(y) = \int_0^{\sqrt{2y}} \frac{xdx}{-1 - \frac{x}{2} + x^3} + \int_{-\sqrt{2y}}^0 \frac{xdx}{-1 - \delta - \frac{x}{2} + x^3}, \quad y \in]0, \frac{x_0^2}{2}[. \quad (57)$$

Following [24, Section 5.3], we know that I_0 has a simple zero $\hat{y}_0 \in]0, \frac{x_0^2}{2}[$, and it follows from the Implicit Function Theorem that this zero persists for $\delta > 0$ sufficiently small. One can compute zeroes of I_0 numerically. Indeed, by approximating the integrand of (57) using Taylor series and then evaluating the integral, one obtains $\hat{y}_0 \approx 0,608853$. Observe that $\frac{x_0^2}{2} \approx 0,679047$.

Now, we define

$$\begin{cases} \dot{x} = y - \frac{x^2}{2}, \\ \dot{y} = \epsilon^2 \left(\epsilon \alpha_- - (1 + \delta)x - \frac{x^2}{2} + x^4 \right), \end{cases} \quad \begin{cases} \dot{x} = y - \frac{x^2}{2}, \\ \dot{y} = \epsilon^2 \left(\epsilon \alpha_+ - x - \frac{x^2}{2} + x^4 \right), \end{cases} \quad (58)$$

with α_{\pm} kept near 0. System (58) with $-$ (resp. $+$) corresponds to the vector field defined in $x \leq 0$ (resp. $x \geq 0$). We have

$$\beta_- = 2(1 + \delta) \text{ and } \beta_+ = 2,$$

with β_{\pm} defined in (50).

Let $\hat{\delta} \in] - \delta_0, \delta_0[$, $\hat{\delta} \neq 0$. Then (58) has no crossing limit cycles Hausdorff close to the balanced canard cycle $\Gamma_{\hat{y}(\hat{\delta})}$, for $\epsilon > 0$, $\epsilon \sim 0$, $\alpha_{\pm} \sim 0$ and $\delta \sim \hat{\delta}$. Indeed, notice that the connection on the blow-up locus between the attracting branch $S_+ = \{y = \frac{x^2}{2}, x > 0\}$ and the repelling branch $S_- = \{y = \frac{x^2}{2}, x < 0\}$ of S is broken, because $\beta_- \neq \beta_+$ for $\delta = \hat{\delta}$ (see Figure 4(a)).

Suppose that $\delta = 0$ and $\alpha_{\pm} = \alpha$. Then (58) becomes a smooth slow-fast system and therefore we are in the framework of [24, Section 5.3]. Thus, for each $\epsilon > 0$ and $\epsilon \sim 0$, (58) undergoes a saddle-node bifurcation of crossing limit cycles, Hausdorff close to $\Gamma_{\hat{y}(0)}$, when we vary $\alpha \sim 0$.

Remark 6. *If $y = \hat{y}$ is a zero of I of multiplicity $m_{\hat{y}}(I)$, then (49) can have at most $m_{\hat{y}}(I) + 1$ limit cycles Hausdorff close to the canard cycle $\Gamma_{\hat{y}}$, for $\epsilon > 0$, $\epsilon \sim 0$ and $\alpha_{\pm} \sim 0$. Moreover, if $\beta_{\pm}(\delta)$ are functions of δ , $\beta_-(0) = \beta_+(0)$ and $\beta'_-(0) \neq \beta'_+(0)$ (connection between p_+ and p_- is broken in a regular way), and I has a simple zero at $y = \hat{y}$, then for each $\epsilon > 0$, $\epsilon \sim 0$ and $\alpha_{\pm} \sim 0$, (49) undergoes a saddle-node bifurcation of (crossing) limit cycles, near $\Gamma_{\hat{y}}$, when we vary $\delta \sim 0$. (We can apply this to (58).) These and other cyclicity results will be proved in a separate paper.*

5.3 Limit cycles near the unbounded canard cycle

Consider the classical PWS Liénard equation

$$\begin{cases} \dot{x} = y - (x^4 + 2x^2), \\ \dot{y} = -\epsilon 2x, \end{cases} \quad x \leq 0, \quad \begin{cases} \dot{x} = y - (x^4 + \delta x^2), \\ \dot{y} = -\epsilon x, \end{cases} \quad x \geq 0, \quad (59)$$

with $\delta \in \mathbb{R}$ kept close to 1. System (59) is a special case of (17) and it satisfies (4) and (6) with $L_- =] - \infty, 0[$ and $L_+ =]0, \infty[$. Statement 1 of Theorem 3.4 implies that, for each δ close to 1, the Minkowski dimension of any entry-exit orbit tending (monotonically) to ∞ is equal to 0.

We focus now on

$$\begin{cases} \dot{x} = y - (x^4 + 2x^2), \\ \dot{y} = \epsilon^2(\epsilon \alpha_- - 2x), \end{cases} \quad x \leq 0, \quad \begin{cases} \dot{x} = y - (x^4 + \delta x^2), \\ \dot{y} = \epsilon^2(\epsilon \alpha_+ - x), \end{cases} \quad x \geq 0, \quad (60)$$

where α_{\pm} are close to zero. We have (see (50))

$$\beta_- = 1 \text{ and } \beta_+ = \frac{1}{\delta}.$$

Take $\hat{\delta} \neq 1$. Then $\beta_- \neq \beta_+$ and (60) has no limit cycles Hausdorff close to the unbounded canard cycle defined in Section 4.3.1, for $\epsilon > 0$, $\epsilon \sim 0$, $\alpha_{\pm} \sim 0$ and $\delta \sim \hat{\delta}$ (see Figure 4(a)). For $\delta = 1$, we have the orbit on the blow-up locus connecting p_+ and p_- (see Figure 4(b)), and the unbounded canard cycle may produce limit cycles of (60) for $\epsilon > 0$, $\epsilon \sim 0$, $\alpha_{\pm} \sim 0$ and $\delta \sim 1$.

Declarations

Ethical Approval Not applicable.

Competing interests The authors declare that they have no conflict of interest.

Authors' contributions All authors conceived of the presented idea, developed the theory, performed the computations and contributed to the final manuscript.

Funding The research of R. Huzak and G. Radunović was supported by: Croatian Science Foundation (HRZZ) grant IP-2022-10-9820. Additionally, the research of G. Radunović was partially supported by the Horizon grant 101183111-DSYREKI-HORIZON-MSCA-2023-SE-01. Otavio Henrique Perez is supported by Sao Paulo Research Foundation (FAPESP) grants 2021/10198-9 and 2024/00392-0.

Availability of data and materials Not applicable.

References

- [1] É. Benoît. Équations différentielles: relation entrée–sortie. *C. R. Acad. Sci. Paris Sér. I Math.*, 293(5):293–296, 1981.
- [2] V. Carmona, S. Fernández-García, and A.E. Teruel. Birth, transition and maturation of canard cycles in a piecewise linear system with a flat slow manifold. *Phys. D*, 443(133566):16, 2023.
- [3] V. Carmona, F. Fernández-Sánchez, and D. D. Novaes. Uniform upper bound for the number of limit cycles of planar piecewise linear differential systems with two zones separated by a straight line. *Applied Mathematics Letters*, 137:108501, 2023.
- [4] Z. Cen and F. Xie. Limit cycles in piecewise smooth van der pol equations. *J. Nonl. Mod. Anal.*, 6(3):732–745, 2024.
- [5] G. Datseris, I. Kottlarz, A.P. Braun, and U. Parlitz. Estimating fractal dimensions: A comparative review and open source implementations. *Chaos: An Interdisciplinary Journal of Nonlinear Science*, 33(10):102101, 10 2023.
- [6] P. De Maesschalck, F. Dumortier, and R. Roussarie. *Canard cycles—from birth to transition*, volume 73 of *Ergebnisse der Mathematik und ihrer Grenzgebiete. 3. Folge. A Series of Modern Surveys in Mathematics [Results in*

Mathematics and Related Areas. 3rd Series. A Series of Modern Surveys in Mathematics. Springer, Cham, [2021] ©2021.

- [7] P. De Maesschalck, R. Huzak, A. Janssens, and G. Radunović. Fractal codimension of nilpotent contact points in two-dimensional slow-fast systems. *Journal of Differential Equations*, 355:162–192, 2023.
- [8] P. De Maesschalck, R. Huzak, A. Janssens, and G. Radunović. Minkowski dimension and slow-fast polynomial Liénard equations near infinity. *Qual. Theory Dyn. Syst.*, 22(4):39, 2023. Id/No 154.
- [9] M. Desroches, E. Freire, Hogan S.J., E. Ponce, and P. Thota. Canards in piecewise-linear systems: explosions and super-explosions. *Proc R Soc A*, 469(2154):18, 2013.
- [10] F. Dumortier. Slow divergence integral and balanced canard solutions. *Qual. Theory Dyn. Syst.*, 10(1):65–85, 2011.
- [11] F. Dumortier and R. Roussarie. Birth of canard cycles. *Discrete Contin. Dyn. Syst. Ser. S*, 2(4):723–781, 2009.
- [12] N. Elezović, V. Županović, and D. Žubrinić. Box dimension of trajectories of some discrete dynamical systems. *Chaos Solitons Fractals*, 34(2):244–252, 2007.
- [13] K. Falconer. *Fractal geometry*. John Wiley and Sons, Ltd., Chichester, 1990. Mathematical foundations and applications.
- [14] S. Fernández-García, M. Desroches, M. Krupa, and A.E. Teruel. Canard solutions in planar piecewise linear systems with three zones. *Dyn. Syst.*, 31(2):173–197, 2016.
- [15] A.F. Filippov. *Differential Equations with Discontinuous Righthand Sides*. Mathematics and its Applications. Kluwer Academic Publishers, 1988.
- [16] U. Freiberg and S. Kohl. Box dimension of fractal attractors and their numerical computation. *Communications in Nonlinear Science and Numerical Simulation*, 95:105615, 2021.
- [17] E. Freire, E. Ponce, and F. Torres. Planar filippov systems with maximal crossing set and piecewise linear focus dynamics. *Springer Proceedings in Mathematics and Statistics*, 54:221–232, 2013.
- [18] M. Guardia, T.M. Seara, and M.A. Teixeira. Generic bifurcations of low codimension of planar filippov systems. *J. Differential Equations*, 250(4):1967–2023, 2011.
- [19] S. M. Huan and X. S. Yang. On the number of limit cycles in general planar piecewise linear systems of node-node types. *J. Math. Anal. Appl.*, 411(1):340–353, 2014.
- [20] R. Huzak. Box dimension and cyclicity of canard cycles. *Qual. Theory Dyn. Syst.*, 17(2):475–493, 2018.

- [21] R. Huzak, V. Crnković, and D. Vlah. Fractal dimensions and two-dimensional slow-fast systems. *J. Math. Anal. Appl.*, 501(2):Paper No. 125212, 21, 2021.
- [22] R. Huzak and P. De Maesschalck. Slow divergence integrals in generalized Liénard equations near centers. *Electron. J. Qual. Theory Differ. Equ.*, 2014:10, 2014. Id/No 66.
- [23] R. Huzak and K. Uldall Kristiansen. The number of limit cycles for regularized piecewise polynomial systems is unbounded. *J. Differ. Equations*, 342:34–62, 2023.
- [24] R. Huzak and D. Vlah. Fractal analysis of canard cycles with two breaking parameters and applications. *Commun. Pure Appl. Anal.*, 18(2):959–975, 2019.
- [25] M. Klimeš, P. Mardesić, G. Radunović, and M. Resman. Reading analytic invariants of parabolic diffeomorphisms from their orbits, 2025.
- [26] M. L. Lapidus, G. Radunović, and D. Žubrinić. *Fractal zeta functions and fractal drums*. Springer Monographs in Mathematics. Springer, Cham, 2017. Higher-dimensional theory of complex dimensions.
- [27] M. L. Lapidus and M. van Frankenhuijsen. *Fractal Geometry, Complex Dimensions and Zeta Functions: Geometry and Spectra of Fractal Strings*. Springer New York, 2013.
- [28] J. Llibre, M. Ordóñez, and E. Ponce. On the existence and uniqueness of limit cycles in planar continuous piecewise linear systems without symmetry. *Nonlinear Anal., Real World Appl.*, 14(5):2002–2012, 2013.
- [29] J. Llibre, M. A. Teixeira, and J. Torregrosa. Lower bounds for the maximum number of limit cycles of discontinuous piecewise linear differential systems with a straight line of separation. *International Journal of Bifurcation and Chaos*, 23(4):1350066, 2013.
- [30] P. Mardešić, G. Radunović, and M. Resman. Fractal zeta functions of orbits of parabolic diffeomorphisms. *Anal. Math. Phys.*, 12(5):70, 2022. Id/No 114.
- [31] P. Mardešić, M. Resman, J.-P. Rolin, and V. Županović. Tubular neighborhoods of orbits of power-logarithmic germs. *J. Dyn. Differ. Equations*, 33(1):395–443, 2021.
- [32] P. Mardešić, M. Resman, and V. Županović. Multiplicity of fixed points and growth of ε -neighborhoods of orbits. *J. Differential Equations*, 253(8):2493–2514, 2012.
- [33] L.V. Meisel and M.A. Johnson. Convergence of numerical box-counting and correlation integral multifractal analysis techniques. *Pattern Recognition*, 30(9):1565–1570, 1997.
- [34] C. Panigrahy, A. Seal, N.K. Mahato, and D. Bhattacharjee. Differential box counting methods for estimating fractal dimension of gray-scale images: A survey. *Chaos, Solitons & Fractals*, 2019.

- [35] I. Pershin, D. Tumakov, and A. Markina. Parallel box-counting method for evaluating the fractal dimension of analytically defined curves. In V. Voevodin and S. Sobolev, editors, *Supercomputing*, pages 86–97, Cham, 2020. Springer International Publishing.
- [36] G. Radunović, D. Žubrinić, and V. Županović. Fractal analysis of Hopf bifurcation at infinity. *Int. J. Bifurcation Chaos Appl. Sci. Eng.*, 22(12):15, 2012. Id/No 1230043.
- [37] M. Resman. ε -neighborhoods of orbits and formal classification of parabolic diffeomorphisms. *Discrete Contin. Dyn. Syst.*, 33(8):3767–3790, 2013.
- [38] A. Roberts. Canard explosion and relaxation oscillation in planar, piecewise-smooth, continuous systems. *SIAM J. Appl. Dyn. Syst.*, 15(1):609–624, 2016.
- [39] J. Ruiz de Miras. Fast differential box-counting algorithm on gpu. *J. Supercomput.*, 76:204–225, 2020.
- [40] C. Tricot. *Curves and fractal dimension*. Springer-Verlag, New York, 1995. With a foreword by Michel Mendès France, Translated from the 1993 French original.
- [41] J. Wu, X. Jin, S. Mi, and J. Tang. An effective method to compute the box-counting dimension based on the mathematical definition and intervals. *Results in Engineering*, 6:100106, 2020.
- [42] D. Žubrinić and V. Županović. Fractal analysis of spiral trajectories of some vector fields in \mathbb{R}^3 . *C. R. Math. Acad. Sci. Paris*, 342(12):959–963, 2006.
- [43] D. Žubrinić and V. Županović. Fractal analysis of spiral trajectories of some planar vector fields. *Bull. Sci. Math.*, 129(6):457–485, 2005.
- [44] D. Žubrinić and V. Županović. Poincaré map in fractal analysis of spiral trajectories of planar vector fields. *Bull. Belg. Math. Soc. Simon Stevin*, 15(5, Dynamics in perturbations):947–960, 2008.